# CHARACTERIZATION OF A 1-D SMALL-PHASED-ARRAY-FED DISCRETE LENS ARRAY (SPAF-DLA)

by
Rita Jakelyn Abad Lima

A thesis submitted in partial fulfillment of the requirements for the degree of

MASTER OF SCIENCE
in
ELECTRICAL ENGINEERING

UNIVERSITY OF PUERTO RICO
MAYAGÜEZ CAMPUS
2017

Approved by:

| | |
|---|---|
| _____ | _____ |
| Rafael A. Rodríguez Solís, Ph.D.<br>President, Graduate Committee | Date |
| _____ | _____ |
| Domingo Rodríguez, Ph.D.<br>Member, Graduate Committee | Date |
| _____ | _____ |
| Shawn D. Hunt, Ph.D.<br>Member, Graduate Committee | Date |
| _____ | _____ |
| Rafael H. Medina Sanchez, Ph.D.<br>Member, Graduate Committee | Date |
| _____ | _____ |
| Roxana M. Barrios Rosales, Ph.D.<br>Representative of Graduate Studies | Date |
| _____ | _____ |
| José G. Colom Ustáriz, Ph.D.<br>Chairperson of the Department | Date |

# ABSTRACT

In this thesis, the characterization of the Small-Phased-Array-Fed Discrete Lens Array (SPAF-DLA) was developed, for the purpose of analyzing an alternative architecture to improve antenna array technology. SPAF-DLA is composed of a small phased array (as feeder) and a discrete lens array (as aperture lens). The purpose of the characterization is to determine the quality of the radiation pattern; the following parameters will be examined: the gain (G), the minimum side lobe level (SLL), the narrowest possible half-power beamwidth (HPBW), the scanning range (SR), and the power distribution in the SPAF. In order to obtain an optimum power distribution, the phase and amplitude in the feeder (i.e. SPAF) was calculated for a given radiation pattern, through of an algorithm optimization. In additional, two synthesis methods were developed and analyzed for the characterization of the SPAF-DLA. As a result, the comparison of 1-D SPAF-DLA's performance with respect to a PHA and a passive DLA (feeders on its focal arc) to compute the cost effectiveness of each structure, with respect to its construction and operating power.

# RESUMEN

En esta tesis, se desarrolló la caracterización del Small-Phased-Array-Fed Discrete Lens Array (SPAF-DLA), con el fin de analizar una arquitectura alternativa para mejorar la tecnología de la matriz de antenas. SPAF-DLA se compone de una pequeña matriz en fase (como alimentador) y una matriz de lente discreta (como lente de apertura). El propósito de la caracterización es determinar la calidad del patrón de radiación; Se examinarán los siguientes parámetros: la ganancia (G), el nivel mínimo de los lóbulos laterales (SLL), la anchura de haz a 3 dB de potencia (HPBW) más estrecha posible, el rango de exploración (SR) y la distribución de potencia en el SPAF. Con el fin de obtener una distribución de potencia óptima, se calculó la fase y la amplitud en el alimentador (es decir, SPAF) para un patrón de radiación dado, a través de una optimización del algoritmo. Además, dos métodos de síntesis fueron desarrollados y analizados para la caracterización de SPAF-DLA. Como resultado, la comparación del desempeño del SPAF-DLA 1-D con respecto al PHA y al DLA pasivo (alimentadores en su arco focal) para calcular la rentabilidad de cada estructura, con respecto a su potencia de construcción y operación.

*This thesis is dedicated to my*

*parents Rita and Reynaldo,*

*my sister Nataly and brother Leonard.*

# ACKNOWLEDGEMENTS

I would like to express the appreciation to my major professor Dr. Rafael A. Rodríguez Solís, who supported me continually in this research. Since without his guidance this thesis would not have been possible. I would like to thank my thesis committee members, Professor Domingo Rodríguez, Professor Shawn David Hunt and Professor Rafael H. Medina Sanchez for their helpful suggestions and comments during my study. I would also like to thank my graduate counselor Sandra Montalvo for all the guidance and moral support through these years.

In addition, I want to thank all of my DSPs lab mates for their support, and cooperation. Finally, I want to express thanks to my family, especially my mother for her constant source of inspiration and support.

# TABLE OF CONTENTS

# LIST OF TABLES

# LIST OF FIGURES

# GLOSSARY OF TERMS

| | |
|---|---|
| AP | Array Pattern |
| AEP | Array Element Pattern |
| AF | Array Factor |
| CLA | Constrained Lens Array |
| dB | Decibels |
| DLA | Discrete Lens Array |
| G | Gain |
| GHz | Giga Hertz |
| HPBW | Half-Power beamwidth |
| $k$ | Free space propagation constant |
| PHA | Phased Array |
| RF | Radio Frequency |
| SFAL | Space Fed Lens Array |
| SLL | Side Level lobe |
| SPAF | Small Phase Array Fed |
| SR | Scanning Range |
| PW | Power |

# 1 INTRODUCTION

Antenna arrays is one of the most important technologies in our present due to the great number of applications on diverse areas such as medicine, communications, remote sensing, and geophysics [1, 2]. A well-known type of antenna array is the Phased Array (PHA), which can achieve beam agility, and flexibility to complex signal environments [2, 3]. However, PHA has some disadvantage and limitations due to its great number of elements, such as high cost, complex array architecture, problems associated with high density device integration, and heat removal [1].

One alternative for replacing the high cost and the complexity of PHA is a Discrete Lens Array (DLA). A DLA is composed of two planar arrays interconnected by transmission-line elements. The lenses are fed by antennas located on the lens focal surface [4]. DLAs replace a large number of expensive phase shifters (i.e. PHA components) with a single spatial feed network, and it avoids the high complexity of the feed network required for PHA [5, 6]. As a result, DLA has not energy distribution and it is a limited-scanning system.

This thesis proposes the characterization of a novel architecture named Small-Phased-Array-Fed DLA (SPAF-DLA), with the idea of analyzing the complexity and the effective cost of this architecture.

## 1.1 Justification

PHAs have a great number of applications (e.g., radar, sonar, surveillance, satellite, airborne, etc.), but it is a very expensive technology [7, 8]. About 50-60% of its cost is due to RF transceivers (i.e. T/R modules), and about 70% of the RF transceiver cost is due to the phase shifters [9, 10, 11]. As reported in [10], a RF transceiver can cost about $300. In this case, a 1.0 $m^2$ PHA at 10 GHz with a rectangular lattice and half wavelength spacing would have about 60x60 (i.e. 3600) elements. The total cost of the full array would be in the order of $1.8M and $2.2M, with the rf transceivers representing about $1.0M of the total cost. The phase-shifters would cost about $700,000, or about a third of the total phased array cost.

DLAs replace the expensive transceivers with a single spatial feed network [14]. For a PHA, power loss increases with array size, whereas than power loss in a DLA is nearly independent of the number of elements, in systems with more than 50 elements, which is a desirable feature for large apertures [12]. Nevertheless, DLAs require a power switching network to point the beam to the desired location, and there is no power distribution in the feed. This means that there is a single point of failure in the system; if the transceiver in the feed fails, so does the antenna. In addition, the size of the power amplifier required in the feed would be much larger than the power amplifiers needed in a conventional array.

In this thesis we will perform the characterization of a novel architecture known as Small-Phased-Array-Fed DLA (SPAF-DLA), because it consists of a passive DLA, and a PHA as a spatial fed network, as shown in Figure 1-1. This architecture is proposed with the

idea of providing a way for spatial power combining at the feed level of the DLA, keeping the lens completely passive, eliminating the need for a high power switching network, and avoiding a single point of failure for the feed. In addition, the use of this proposed architecture in place of a phased-array antenna would require a much smaller number of microwave transceivers, simplifying the control system required, and reducing costs. For instance, a small 6x6 PHA (36 elements) should cost around $20,000. From this total, about $10,000 would be due to the transceivers. Since the DLA is completely passive, it can be manufactured inexpensively with standard photolithographic techniques. In addition, this thesis will provide a radiation pattern synthesis procedure, a characterization of the novel architecture, and a comparison of the proposed architecture with a conventional DLA and the PHA.

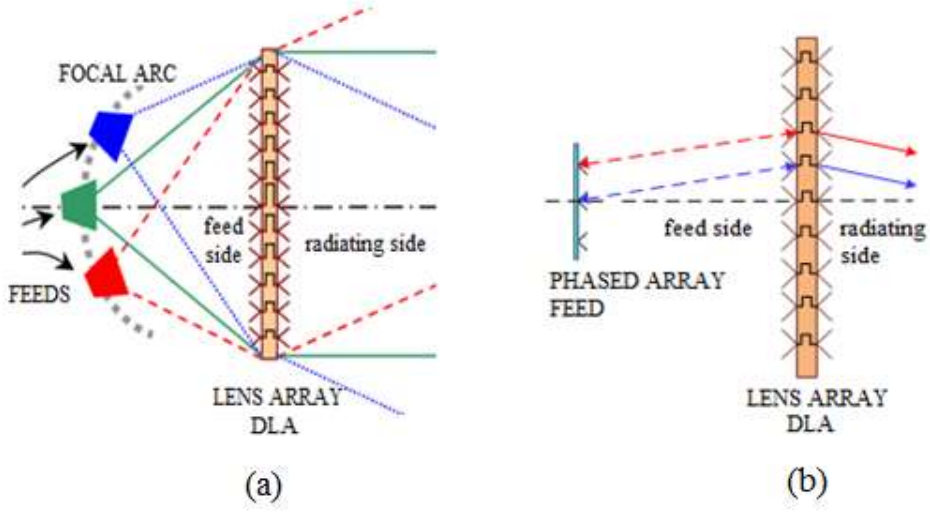


**Figure 1-1.** Schematic of a DLA with (a) three independent feeds on its focal arc, and (b) Small-Phased-Array-Fed DLA (SPAF-DLA).

## 1.2 Objectives

The main objective of this thesis research is to characterize a 1-D Small-Phased-Array-Fed DLA (SPAF-DLA). The SPAF size will be limited to be around 10 times smaller than the size of the DLA. The purpose of the characterization is to determine the quality of the radiation pattern; the following parameters will be examined: the gain (G), the minimum side lobe level (SLL), the narrowest possible half-power beamwidth (HPBW), the scanning range (SR), and the power distribution in the SPAF.

### 1.2.1 Specific Objectives

1. Characterize a 1-D Small-Phased-Array-Fed DLA (SPAF-DLA) to obtain the radiation patterns for different positions of the Small-Phased-Array-Fed (SPAF) with respect to DLA, and the element distribution and number of elements in the feed (i.e. SPAF).
2. Compute power distribution in the feeder (i.e. SPAF), through of the optimization of phase and amplitude for a given radiation pattern.
3. Compare the performance of the 1-D SPAF-DLA with respect to a PHA and a passive DLA (feeders on its focal arc) to compute the cost effectiveness of each structure, with respect to its construction and operating power.

## 1.3 Contribution to the Scientific Community

This thesis will make a contribution to the scientific community, by providing a novel alternative, namely a Small-Phased-Array-Fed DLA (SPAF-DLA), to improve antenna array technology. As a result, SPAF-DLA is expected to reduce costs compared to a PHA and provide power combining capabilities at the feed of a DLA.

## 1.4 Thesis Organization

This thesis describes the design and characterization for a 1-D Small-Phased-Array-Fed DLA (SPAF-DLA). It also analyzes the power distribution in the feed to compare its performance to a phased array PHA and a discrete lens array DLA.

A brief theoretical background and literature review is presented in Chapter 2. Thus, this chapter presents a short description of the basic definitions used in the theory of linear phased arrays, array performance metrics, and Constrained Lens Arrays (CLA). In addition, a literature review on state-of the-art antenna arrays is given, as well as a description of the thesis contribution.

Chapter 3 presents the methodology used for the analysis, design and simulation of the algorithms that are going to characterize SPAF-DLAs. It also explains their development process, as well as an optimization algorithm to observe which parameter values will give better and/or similar estimations. Additionally, this chapter defines the parameters to be

used to calculate the algorithms, the limitations and advantages of each of the variables, and explains the importance of these algorithms to help to characterize SPAF-DLA.

Chapter 4 provides the simulations and results of the SPAF-DLA characterization. The scanning performance of several array parameters, including Side Level Lobes (SLL), Half-Power beamwidth (HPBW), directivity (D), Scanning Range (SR) and Power (PW) are shown compared to others systems, such as DLA and linear phased array. Finally, this chapter evaluates the SPAF-DLA architecture as a low-cost alternative, compared to a linear phased array and discrete lens array. Finally, chapter 5 summarizes the conclusions obtained in this thesis work.

# 2 LITERATURE REVIEW

A brief description of the basic definitions used in the theory of linear PHA, array performance metrics, and Constrained Lens Array (CLA) will be presented in this section. In addition, a literature review of development and applications antenna array is presented, and the contribution this thesis described.

## 2.1 Theoretical Background

### 2.1.1 Antennas Array

An antenna array is a configuration of multiple antennas (elements) arranged to achieve a given radiation pattern, i.e. a linear array is composed of antenna elements arranged along a straight line. An antenna array also can be enabled to be electronically steered - to receive or transmit information primarily from a particular direction without mechanically moving the structure [15].

There are several antenna array design variables, which can be changed to achieve the overall array pattern design. Antenna arrays have the following main design variables:

1. General array shape (linear, circular, planar, etc.).

2. Element spacing ($d$).

3. Element excitation amplitude ($A_n$).

4. Element excitation phase ($\emptyset_n$).

5. Array element pattern (AEP).

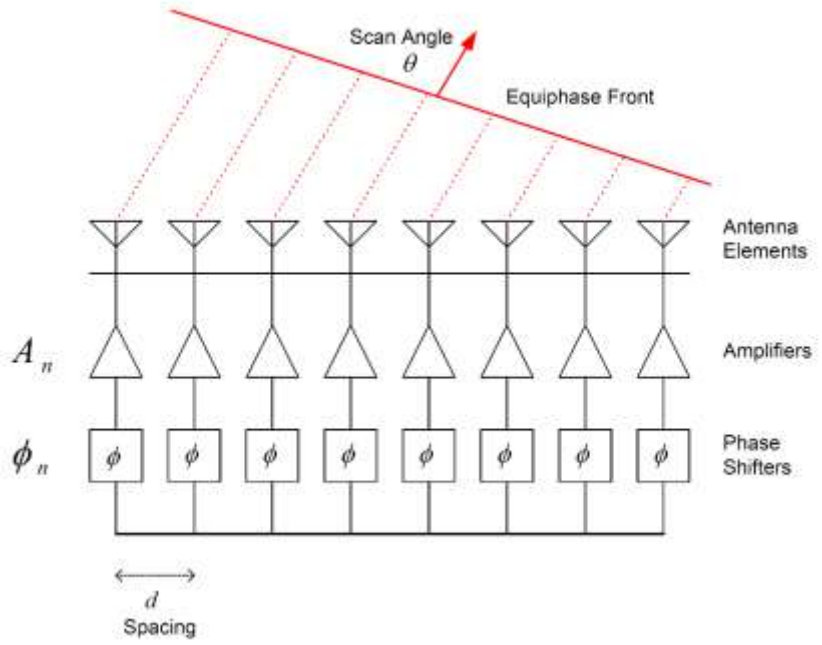


**Figure 2-1.**Block diagram of an antenna array, i.e. phased array (PHA).

Given an antenna array of identical elements and without mutual coupling, the radiation pattern of the antenna array may be found according to the pattern multiplication theorem. The pattern multiplication theorem is described in equation (2.1), where the array pattern (AP) is the multiplication of the array element pattern (AEP) and the array factor (AF). The AEP represents the pattern of the individual array element, whereas the AF is a function

that depends only on the geometry of the excitation (amplitude $A_n$ and phase $\emptyset_n$) of the elements. The AP can be calculated using the following equation:

$$\mathrm{AP} = \mathrm{AEP} \times \mathrm{AF} \qquad (2.1)$$

#### 2.1.1.1 Periodic Array

Most antenna arrays are periodic arrays, in which the individual spacing between elements have the same spacing, usually range from 0.5 up to 0.7 wavelengths. Element spacings greater than 0.5 wavelengths may cause grating lobes to enter the visible region when the main beam is scanned beyond a specific angle from broadside.

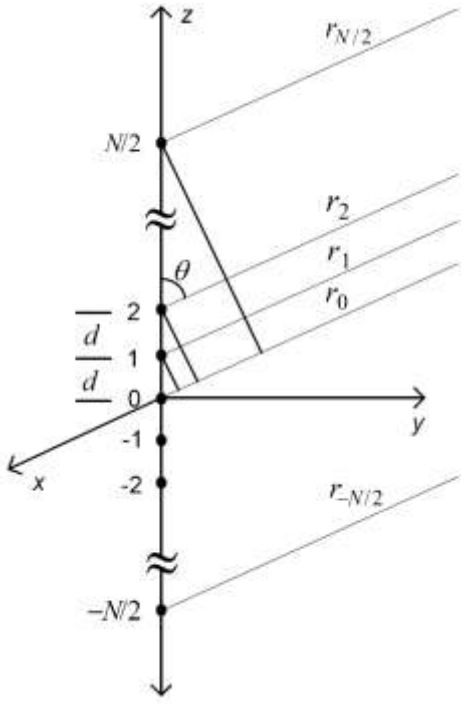


**Figure 2-2.**Typical one-dimension periodic array with element spacing, $\boldsymbol{d}$.

Let us assume that an array of $N+1$ elements placed along the z- axis separated by a spacing equal to $d$, which is shown in Figure 2-1. The array factor (AF) is independent of array element pattern (AEP). Thus, isotropic radiators may be utilized in the derivation of the AF to simplify the algebra. In equation (2.2), $k$ is the free space propagation constant at the operating frequency, $r_n$ is the distance of each element to the observation point, and $\theta$ is the far-field observation angle. $I_0$, it is the current magnitude on the array element located in the origin. The field of an isotropic radiator, $E_n(\theta)$, located at the origin of the z-axis may be written as (assuming $\theta$-polarization):

$$\mathrm{E_n(\theta) = I_0 \frac{e^{-jkr_n}}{4\pi r_n}};\quad n = -N/2, \cdots, 0, 1, \cdots, N/2 \qquad (2.2)$$

In the far field of a periodic array, i.e. that the elements of the array are uniformly spaced with a separation distance $d$,

$$r_n = r_0 - nd\cos\theta \qquad (2.3)$$

The amplitude $A_n$ and phase $\emptyset_n$ contribution of each individual element in a transmitting array is summed across the visible region. Equation (2.4) describes the general form for calculating the array factor (AF) of a periodic array [16]. This equation assumes point sources as the antenna element and no mutual coupling effects between elements. The terms, $\emptyset_n$, represent the phase shifts from the elements to a point in space due to propagation (usually in the far field). The far-fields of the individual array elements are:

$$AF = \sum_{n=-N/2}^{N/2} e^{j(\emptyset_n + kd\cos\theta)} \tag{2.4}$$

This is an uniform linear array of $N+1$ elements with uniform spacing, uniform amplitude and linear phase progression in equation (2.5), which is defined by uniformly-spaced identical elements of equal magnitude $d$ with a linearly progressive phase $\alpha$ from element to element, can be determined by:

$$\phi_1 = 0 \quad \phi_2 = \alpha \quad \phi_3 = 2\alpha \quad \cdots \quad \phi_N = (N-1)\alpha \tag{2.5}$$

Substituting equation (2.5) in equation (2.4), the phase can be redefined by equation (2.6), and the factor can be rewritten as equation (2.7).

$$\psi = \alpha + kd\cos\theta \tag{2.6}$$

$$AF = \sum_{n=-N/2}^{N/2} e^{j(n+1+N/2)\psi} \tag{2.7}$$

The function $\psi$ is defined as the array phase function. The array phase function is a function of the element spacing $d$, phase shift $\alpha$, frequency and $\theta$.

#### 2.1.1.2 Aperiodic Array

Aperiodic arrays are antenna arrays in which the spacing between elements is irregular across the aperture (i.e. different spacing between elements). This provides many advantages over the periodic counterpart, for instance, aperiodic arrays can allow multiple frequencies of operation without sacrificing pattern performance. The average spacing between elements can exceed a 0.5 wavelength and simultaneously eliminate the grating lobe that would appear in the periodic array. Because of this larger average inter-element spacing, aperiodic arrays can be designed to require fewer elements than the periodic array. This reduction in antenna elements can reduce the weight and cost of the system in large array applications [17].

In the previous section, equation (2.4) and (2.7) presented a simplified array factor (AF) for periodically spaced antenna arrays. Unfortunately, the additional degree of freedom associated with aperiodic arrays does not allow one to use this simplified formula. The AF for a linear aperiodic array of $N + 1$ elements must be calculated as a summation of fields [18] using the following equation:

$$AF = \sum_{n=-N/2}^{N/2} e^{j(\emptyset_n + kd_n \cos\theta)} \tag{2.8}$$

The variable spacing between elements, $d_n$, does not allow for this equation to be simplified as in the periodic case. These arrays are very difficult to evaluate analytically and in very large arrays, designing them can be computationally strenuous. These

inconveniences have created an interest in finding alternative techniques to analyze these aperiodic arrays.

### 2.1.2 Array Performance Metrics

As with all antennas, the performance of an antenna array can be measured using several metrics. Some of the most important metrics that will be used in this thesis work are the gain (G), half-power beamwidth (HPBW), side lobe level (SLL) and scanning range (SR). The gain is the characteristic of an antenna that describes how much it concentrates energy in one direction in preference to radiation in other directions [19, 20]. Directivity (or maximum directivity) is an important antenna parameter that describes how much more directional an antenna is from a reference source, usually an isotropic radiator. An antenna with a directivity of 1 (or 0 dB) would be an isotropic source; all actual antennas exhibit directivity higher than this. By definition, the directivity is given as the ratio of the radiation intensity in a certain direction to the average radiation intensity, or:

$$D = \frac{4\pi}{\int_0^{2\pi}\int_0^{\pi}[f(\theta,\emptyset)]^2 \sin\theta \, d\theta d\emptyset} \tag{2.9}$$

where $f(\theta,\emptyset)$ is the normalized field pattern of the antenna.

Beamwidth is commonly defined as the half-power beamwidth (3 dB beamwidth) or (HPBW) [21]. This is a measure of the angular separation of points where the main beam

is equal to one-half of its maximum value, or -3 dB relative to the normalized maximum gain of the beam, 0 dB.

The side lobe level (SLL) is the difference between the peak gain of the amplitude main lobe and the peak gain of the maximum side lobe. This represents how well the power is concentrated into the main lobe [21]. In a periodic array the maximum side lobe will always be the one closest to the main beam, called the first side lobe [20]. An array antenna to a determined frequency can steer its beam in different directions. The sweep that makes the beam of an antenna array, is known as scanning range (SR), which can vary depending on the design of the array.

Furthermore, in a periodic array, if the elements are driven in phase to produce a broadside beam, the AF always produces a symmetrical pattern, independent of the amplitude distribution on the array. Scanning the beam away from broadside maintains a symmetrical beam shape so long as the phase shift between elements has a linear progression.

### 2.1.3 Constrained Lens Array (CLA)

Constrained Lens Arrays (CLA) share some similarities with the dielectric lenses and reflector antennas on one hand and with antenna arrays on the other. Their function is to form beams in multiple directions which correspond to the location of the feed antennas at the focal surface [22]. The name constrained comes from the fact that a wave incident on one face of the array does not necessarily obey Snell's law when passing through the lens array; it is instead constrained to follow the transmission line paths [23].

#### 2.1.3.1 Microstrip Constrained Lens Array (McGrath Lens)

A CLA with planar front and back faces, which uses only two degrees of freedom was first proposed by McGrath [ 24, 25], and is also commonly known as Discrete Lens Array (DLA). He suggested arrays of microstrip patch antennas with a common ground plane, and delay lines made with microstrip transmission lines. Connection between the elements on two sides of the array can be either a feed-through pin or a slot coupler in the ground plane.

The derivation of the lens design equations follows. A linear lens is considered first as shown in Figure 2-3. In order to design a lens with two focal points located at $(y, z) = (-F\cos\theta_0, \pm F\sin\theta_0)$, two equations have to be satisfied:

$$\sqrt{F^2 + \rho^2 - 2\rho F \sin\theta_0} + W + r\sin\theta_0 = F + W_0 \qquad (2.10)$$

$$\sqrt{F^2 + \rho^2 + 2\rho F \sin\theta_0} + W - r\sin\theta_0 = F + W_0 \qquad (2.11)$$

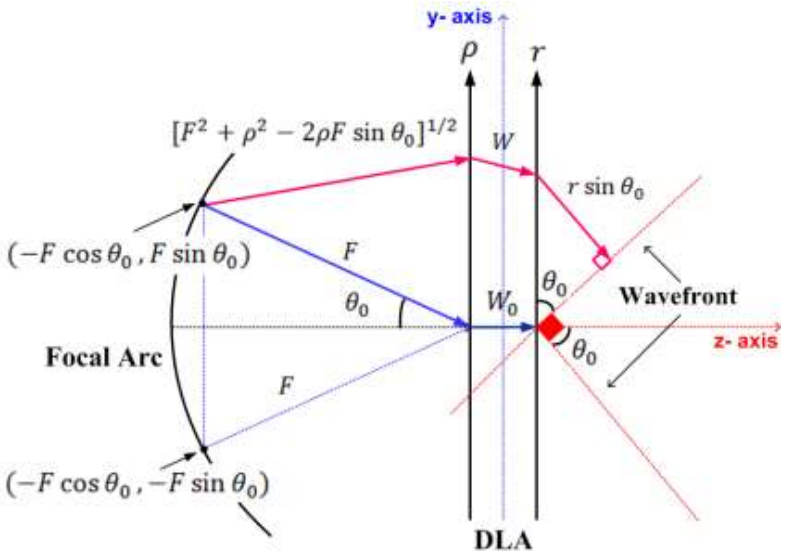


**Figure 2-3.**Linear constrained lens array with two degrees of freedom.

where $F$ is the focal length of the delay lines, $W_0$ is an arbitrary constant, and $r$ and $\rho$ are the coordinates of the antenna elements at the non-feed side and the feed side of the lens array. Solving these two equations for $\rho$ and $W$ gives:

$$\rho = r\sqrt{\frac{F^2 - r^2 \sin\theta_0{}^2}{F^2 - r^2}} \tag{2.12}$$

$$W = F + W_0 - \frac{1}{2}\sqrt{F^2 + \rho^2 - 2\rho F\, sin\,\theta_0} - \frac{1}{2}\sqrt{F^2 + \rho^2 + 2\rho F\, sin\,\theta_0} \tag{2.13}$$

## 2.2 Literature Review

### 2.2.1 Phased Array antenna

PHA antenna is a very expensive technology by cause of the phase shifters [22]. As the technology advances, costs are expected to be reduced [26], however, the quest for better performance with lower side lobes and wider bandwidth has kept their cost high [24].

Most applications and researches use PHA antenna are diverse; for example, the National Center for Atmospheric Research (NCAR) [27] has investigated several potential phased array radar configurations for a next-generation airborne research radar, two U.S. Navy surveillance phased-array radars have been modified for use as weather radars [28]. The first one is the National Weather Radar Testbed (NWRT) operated by the NOAA National Storm Severe Laboratory (NSSL) [29,30,31] and the second is the Mobile Weather Radar, 2005 X-Band, Phased Array (MWR-05XP) operated by Processing [32,33].

Although PHAs claim many advantages [20, 21, 22], they also have some disadvantages in certain applications [23, 24]. Most PHAs are periodic arrays, which require equal spacing between elements [25], which causes problems for some applications such as wideband array applications. To avoid an unsuitable performance in wideband applications, the spacing between elements must be large, usually greater than 0.5 wavelength [26]. Depending on the desired bandwidth of the array, the spacing between elements can exceed 1.0 wavelength. If this occurs, grating lobes appear in the visible region, making the tracking of targets virtually impossible [27, 28].

Another disadvantage to periodic arrays is that in order to secure high gain and narrow beamwidth, a very large array of elements must be produced [29, 30, 31]. Depending on the frequency of operation, this could require thousands of elements (i.e. radiators or antennas), making the array very expensive to constructed. Because of this, research has been conducted into alternative arrays which would require fewer elements, thus reducing the cost of the PHAs [32].

An alternative to periodic PHA is the aperiodic array, for which the spacing between elements is not equal, but irregular across the array aperture. Researchers [32, 33, 34], claimed that this irregular spacing helped eliminate grating lobes, making aperiodic arrays a prime candidate for high bandwidth applications where scanning is required. Also, the aperiodicity of the array requires fewer elements than the periodic array, drastically reducing the cost of the array [33].

Most investigators [35] attempted to solve the problem using analytical techniques. Several authors were successful, but the technique could only be applied to very small arrays because of the computational complexity [36]. Computing resources at this time are not powerful enough to solve the problem in real time.

Currently aperiodic arrays almost exclusively take advantage of computers power to help solve the problem analytically [22]. Most researchers had limited success with small to moderately sized arrays. Another group of researchers approached the problem using optimization techniques [26, 30].

In conclusion, research today is that solving the problem analytically for large arrays is still very complicated, even with the help of computers. Most researchers have concluded that

the best way to design these arrays is to approach the design as an optimization problem [30,34]. Many optimization algorithms have proven to be successful tools for solving these electromagnetic problems, providing good results in a reasonable amount of time.

### 2.2.2 Discrete Lens Array (DLA)

DLAs are an alternative to dielectric lenses or other technologies, which are too heavy, lossy, and required at least one of the lens surfaces to be curved making fabrication difficult [34, 37]. Since a DLA is constructed as two planar arrays using printed circuit boards, it is referred to as a constrained lens [17]. As a result, the DLA reduces the complexity of design and construction of a lens by avoiding the oval geometry.

Also, the DLA is described as Space Fed Lens Array (SFLA) [35], where it is an alternative for adaptive ground station applications, i.e. multibeam applications [12]. In addition, these papers report that DLAs have lower cost as compared to a PHA, at the expense of total volume and complete beam continuity. For communicating and tracking low Earth orbiting satellites, the dynamic beam steering is achieved through switching to different feed positions of the DLA via a beam controller.

Many multibeam applications use DLA [33,12,37], such as wireless communication and satellite crosslinks [38]. As reported in [39], DLA is presented as a multibeam spatially fed antenna array, where DLA operates at 10 GHz, with a half-power beamwidth that varies by 2 degrees and an apertures lens discrete of 45 elements (a best focus angle at $\pm 45$ degrees) . In other paper, for a satellite communication ground station application [40], DLA is described as an array with around 100 elements at 8.2 GHz (i.e. X-band), and a

scanning range from $\pm 55$ degrees. Also, in other applications as satellite cross links dual-frequency [41], DLA operates at 24.7 GHz and 26.7 GHz, moreover, this DLA is composed of 64 elements and a best focus angle at $\pm 45$ degrees.

Other application of the DLA is in Smart Systems, such as cognitive radar [42]. In these systems, the processing load can be too much huge to standard arrays (i.e. PHAs). Thus, DLA is presented in [43] as an alternative and is described as a smart lens antenna array in which a portion of the signal processing is implemented at the analog front end, resulting in reduced processing load [42, 43].

### 2.2.3 Antenna system consisting of lens antenna and PHA

Generally, an antenna system comprises PHAs and lens antennas, where the latter is commonly a dielectric lens or a discrete lens array (DLA) [17]. For instance, some applications such as satellite communications and collision-avoidance car radars use the dielectrics lens as aperture antenna and simple patch array feeds at 20 GHz; if the patch array is replaced by horn the operation frequency would be 60 GHz [34, 36].

Another system for limited electronic scanning applications proposes a dual lens antenna and a phased array feed [38], however, when this system is assessed to derive the size of the phased-array feed, it is determined that the system has no advantage over a PHA. To avoid the grating lobes in the antenna coverage area, the size of the phased-array feed has to be equal to the size of the aperture lens.

This thesis proposes the synthesis of a system or an architecture conformed by a DLA as a lens aperture and a small PHA as an array feed. The main contribution is the

characterization of the architecture to obtain a suitable energy distribution and localization of the elements on the PHA, according to desired radiation pattern. The following chapter explains in greater detail the architecture.

# 3 METHODOLOGY

In this section is described each stage that was developed for the characterization of the Small-Phased-Array-Feed DLA (SPAF-DLA). It is also explained design SPAF-DLA, analysis, synthesis and their parameters, which are used to observe and obtain the radiation pattern.

## 3.1 Geometrical Description of the Proposed Architecture

The proposed architecture, namely as Small-Phased-Array-Fed DLA (SPAF-DLA), is integrated of a DLA and a PHA. In the case of DLA, it was designed by means Mc. Grath equations [18], DLAs geometry is shown in Figure 3-1. As DLA is composed from two linear arrays on y- axis, i.e., an array in the feed side (FS) and other in the radiation side (RS), where elements positions in the DLA utilize equation (3.1). For N+1 elements on each linear array, being their radial position vectors $\rho_n$ in the feed side and $r_n$ in the radiation side. Beside, $F$ is the focal length and $\pm\theta_0$ is the best focal angle of the DLA, .

$$\rho_n = r_n\sqrt{\frac{F^2 - {r_n}^2 \sin^2(\theta_0)}{F^2 - {r_n}^2}}; \quad n = -N/2, \cdots, 0, 1, \cdots, N/2 \qquad (3.1)$$

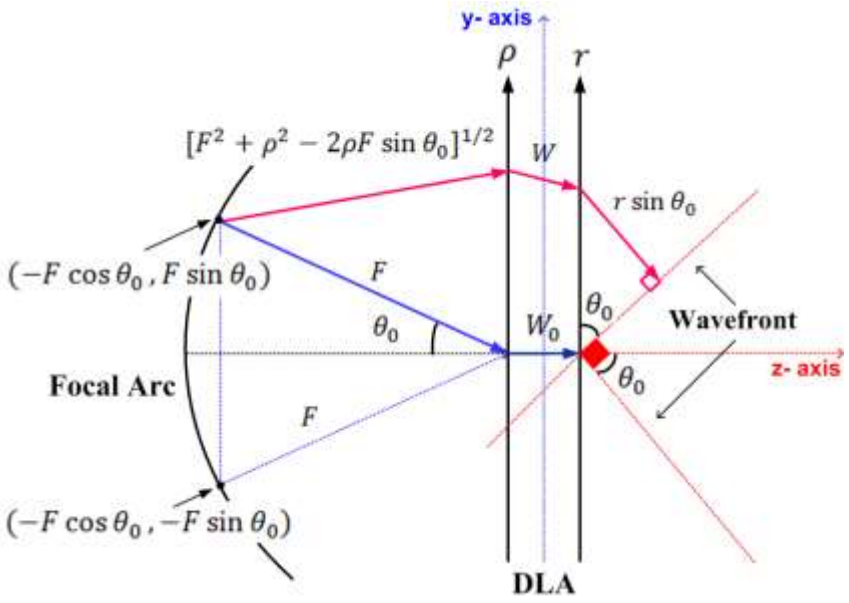


**Figure 3-1.**Linear two degree of freedom (2DF) lens reference geometry-i.e. $\boldsymbol{\rho_n}$ and $\boldsymbol{\theta_0}$.

Continuing with DLA design, the length of transmission line joining elements of opposing linear array (i.e. through a delay or separation), $W_n$, which is determined by equation (3.2). $W_0$ is the constant assigned to the separation among the located elements on the z- axis.

$$W = F + W_0 - \frac{1}{2}\sqrt{F^2 + {\rho_n}^2 - 2\rho_n F \sin\theta_0} - \frac{1}{2}\sqrt{F^2 + {\rho_n}^2 + 2\rho_n F \sin\theta_0} \qquad (3.2)$$

As according to Mc Grath, the design of DLA is constrained to that both inner and outer lens contours are linear. With that limitation, there can be at most two perfect focal points $\pm\theta_0$, however, DLA is used to other focal points by refocusing path length errors for this lens design. Thus, this thesis work analyzes the DLA in how well the lens focuses everywhere else and elements radiation outside the arc focal (i.e. SPAF-DLA).

The geometry of the 1-D Small-Phased-Array-Feed DLA (SPAF-DLA) is shown in Figure 3-2. In equation (3.3), $R_{mn}$, is a matrix of the distances among SPAFs elements and DLAs elements (in the feed side); $s_m$ is the position vector of every element in SPFA; $M+1$ is the number of elements in the SPAF; P is SPAF distance on z- axis with respect to DLA. All element on DLAs feed side have a radiation pattern, $E_{fsn}$, which is calculated as the sum of the electric field, $E_{fm}$, of all element on the SPAF in equation (3.4). $k$, is wavenumber; $m = -M/2, \cdots, -1, 0, 1, \cdots, M/2$ ; $n = -N/2, \cdots, -1, 0, 1, \cdots, N/2$; $k = 2\pi/\lambda$, and $\lambda = 1$.

$$R_{mn} = \sqrt{(P^2 + (\rho_n - s_m)^2)} \tag{3.3}$$

$$E_{fs_n} = \sum_{m=-M/2}^{M/2} E_{fm} \frac{e^{-jkR_{mn}}}{R_{mn}} \tag{3.4}$$

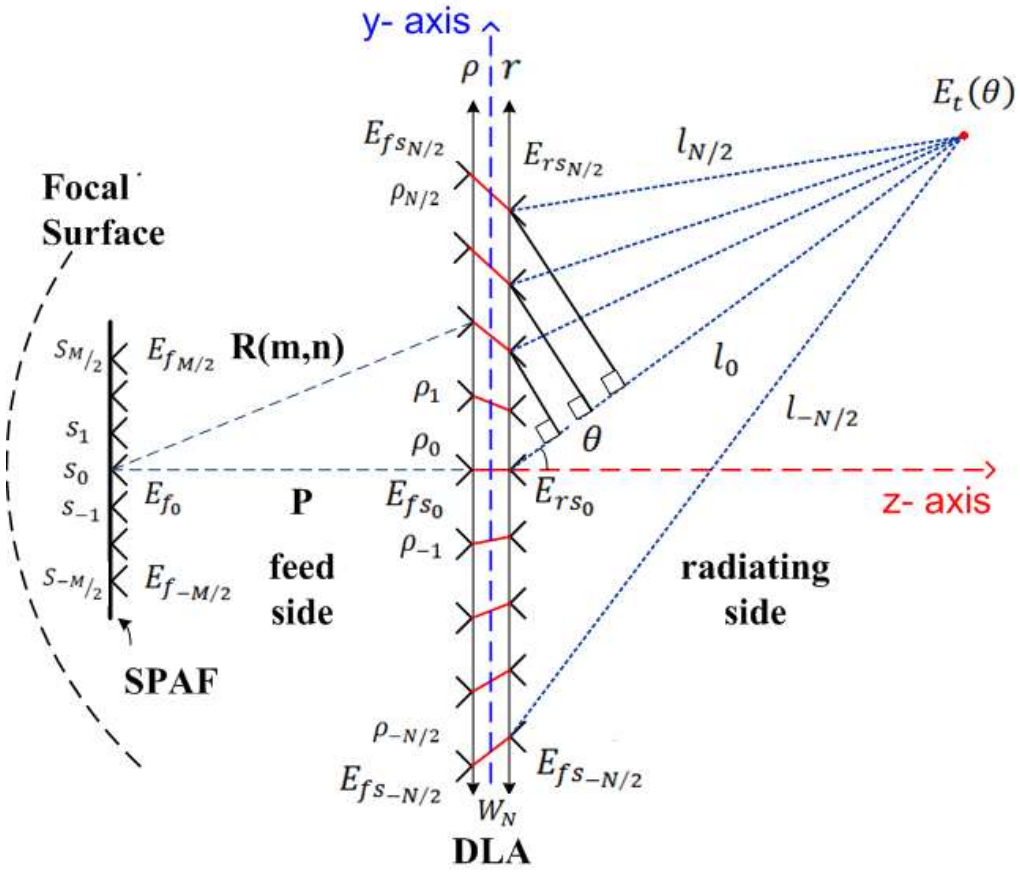


**Figure 3-2.**Geometry of the Small-Phased-Array-Feed DLA (SPAF-DLA) in terms of the variables used in equations (3.3-3.6).

Therefore, the electric field of every element in DLA radiation side, $E_{rsn}$, is the radiation pattern in DLA feed side, $E_{fsn}$, con un delay or separation, $W_n$, as is shown in the following equation:

$$E_{rs_n} = E_{fs_n} W_n \tag{3.5}$$

The electric field for a point of interest $E_t(\theta)$ is determined in equation (3.6); $r_n$ is the position of each element on the radiation side; $\theta$ is the angle at which the point of interest is with respect to the z- axis; $l_0$ is the distance from the element in the center or origin position of the DLA to the point of interest; $l_n$ is the distance from each element of the DLA to the point of interest; $E_{rsn}$ is the radiation pattern for the radiation side of the DLA; $l_n = l_0$; $k = 2\pi/\lambda$, and $\lambda = 1$.

$$E_t(\theta) = \frac{e^{-jkl_0}}{l_0} \sum_{n=-N/2}^{N/2} E_{rs_n} e^{jr_n \sin(\theta)} \tag{3.6}$$

## 3.2 Analysis of the novel architecture performance

The analysis of the architecture performance is divided in two parts: the first part is DLA's design, and the second part is radiation pattern's analysis. Also, it will be detailed the values of some variables such as $N,\ \theta_0, r_n, M, P, s_m$, in next sections respectively.

### 3.2.1 Designed of the DLA

As mentioned in the previous sections the design of the DLA is made from equations by Mc Grath [18], as is shown in Figure 3-3. Therefore, to resolve those equations are required

next parameters values, such as the number of elements in the DLA $N+1$, the angle of best focus $\pm\theta_0$, and finally element's position vector in the radiation side $r_n$.

Because of that element's position is on the z- axis form linear arrays, and to reduce design complexity this linear array also is periodic and the spacing between elements is $0.5\ \lambda$ or half wavelength. This spacing is selected to avoid the introduction of grating lobes while scanning. In the case of the best focal angle, $\theta_0$, is a variable that initially take the value of $20$ degree, because it is an angle that is not very close to or far from the broadside. However, $\theta_0$, takes others values in the analysis and the characterization of SPAF-DLA.

DLA have two linear arrays, each of which contains 65 elements (or $N+1=65$), since it is known that with this number of elements and a spacing of $0.5\ \lambda$ a linear array periodic originates a radiation pattern with SLL (11 dB), HPBW (2 degree), Gain (18 dB) and a range scan of almost $\pm 80$ degrees. This radiation pattern has been a good benchmark of the performance of the new architecture, as is shown in Figure 3-4.

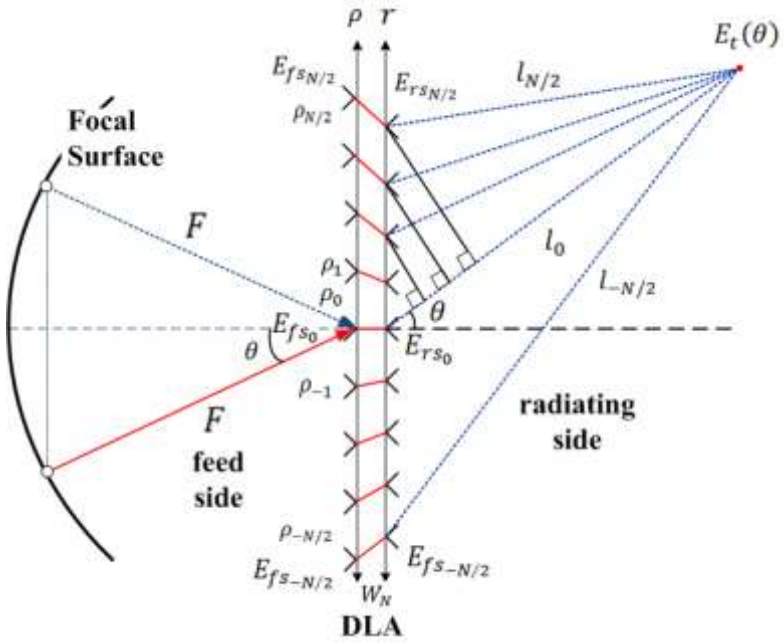


**Figure 3-3.** Geometry of the DLA in terms of the variables used in equations (3.3-3.6).

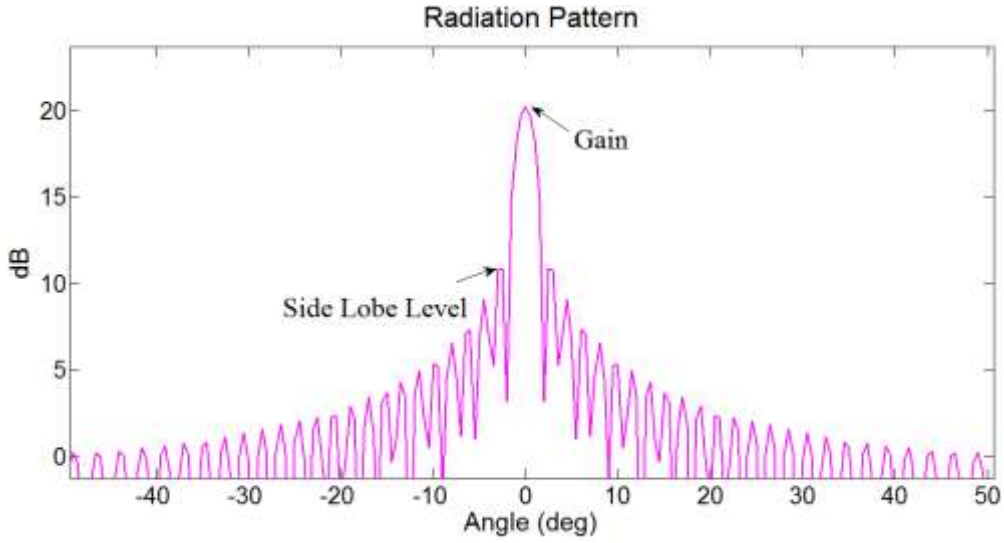


**Figure 3-4.**Obtaining the radiation pattern from the linear array in the radiation side .

### 3.2.2 Analysis of the radiation pattern

After defining the values of the DLA design parameters, the next step is the determination of the values of the SPAF parameters ($M+1, P, s_m$) to perform the radiation pattern's analysis. This analysis assumes that SPAF's elements are identically, which are on the y-axis forming a linear array, and its position vector $s_m$ is located at the position $P$ on the z-axis, as is shown in Figure 3-5. Given that the excitation (amplitude $A_{fm}$ and phase $\phi_{fm}$) in the feeding (i.e. SPAF), and SPAF's electrical field, $E_{f_m}$, is defined as:

$$E_{f_m} = A_{f_m} e^{j\phi_{fm}}; \quad m = -\frac{M}{2}, \cdots, 0, \cdots, \frac{M}{2} \tag{3.7}$$

Because of that one of the objectives was reduced $M+1$ (or elements number of the SPFA), and the ratio of this amount with respect to $N+1$ (or elements number of the DLA) should be approximately 10. Given that $N+1=65$, then the values that $M+1$ taken is $5, 7, 9$. Also, the values of the position vector $s_m$ should not be greater than $D$ the diameter of the DLA, which calculated as:

$$D = N \times r_n \tag{3.8}$$

Replacing the values in equation 3.8, according to the previous section, $N$ has the value of 64 and $r_n$ is half wavelength (or 0.5 $\lambda$), as a result $D$ is equal to 32 $\lambda$. Thus, for assessing the values of $P$, the focal length $F$ is taken as reference, which is in function of diameter $D$, as is shown in equations 3.9. Also, $F$ depends of $\beta$, which initially taken the value equal to 1. In equation 3.10, $P$ is in function of $F$ by means the values of $p$, whose range is of 0.1 to 1.0.

$$F = \beta \times D \tag{3.9}$$

$$P = p \times F \tag{3.10}$$

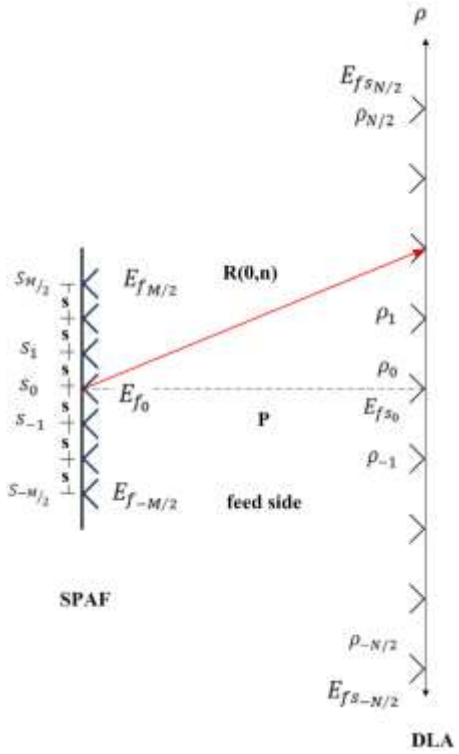


**Figure 3-5.**Small-Phased-Array-Feed SPAF and the feed side of the DLA as a periodic linear array.

Since that the parameters were defined in the previous equations, then the next step is to choose the parameters values and calculate the excitation values (amplitude $A_{fm}$ and phase $\phi_{fm}$) to generated the radiation pattern. This excitation values were calculated from of a MATLAB function of optimization $fminsearch$ or $fminunc$, the algorithm of these function is described in the following equation:

$$\min_{x} f(x); \;\; x\epsilon\chi \tag{3.11}$$

Where $f(x)$ is the objective function to be minimized, and $\chi$ is known as the set of all possible solutions, $x$ is a vector or matrix. The optimal value of $x$ to resolve equation 3.11 is $x_{opt}$, and it have the property:

$$f(x_{opt}) \leq f(x); \quad \forall\, x\epsilon\chi \tag{3.12}$$

In this case, $x$ represents the excitation values, i.e. amplitude $A_{fm}$ and phase $\phi_{fm}$ (radians),

$$x = \begin{bmatrix} A_{f1} \\ A_{f2} \\ \vdots \\ A_{fm} \\ \emptyset_{f1} \\ \emptyset_{f2} \\ \vdots \\ \emptyset_{fm} \end{bmatrix}; \qquad m = 1, \cdots, M+1; \tag{3.13}$$

Also, $f(x)$ is Least Mean Squares (LMS) of the desired radiation pattern $E_d(\theta)$ and the radiation pattern $E_t(\theta)$ obtained from the values of $x$, and $\theta$ is steering angle,

$$f(x) = |E_d(\theta) - E_t(\theta)|^2 \tag{3.14}$$

Given that $E_t(\theta)$ is obtained as:

$$E_t(\theta) = \frac{e^{-jkl_0}}{l_0} \sum_{n=-N/2}^{N/2} E_{rs_n} e^{jr_n \sin(\theta)} \tag{3.15}$$

Also,

$$E_d(\theta) = \sum_{n=-N/2}^{N/2} \left[1 + \cos\left(\frac{n\pi}{N}\right)\right] e^{-jk\, r_n \sin\theta} \tag{3.16}$$

Equations (3.11-3.16) calculate the minimum error using the MATLAB Optimization Toolbox- to obtain optimum amplitude and phase of the elements in the feed side of the DLA.

### 3.2.2.1 Periodic elements distributions of the SPAF

Given that the excitation in the SPAF ($E_{fm}$) is optimized for each values of the parameters $s_m$, $P$, $M+1$. Then, the radiation pattern is assessed according to changes of $p$ for the fixed values of $M+1=7$, $F=32\ \lambda$ and as it is a periodic array all values of the $s_m$ are equal, in this case $s_m=0.5\ \lambda$. Figure 3-6 and 3-7 shown as the radiation pattern varies when $p$ takes the values of 0.1 and 0.5, i.e. for $P$ equal to $3.2\ \lambda$ and $16\ \lambda$. Also, in Figure 3-8 shown as the radiation pattern for $P=16\ \lambda$ and $s_m$ takes the values of $0.1\ \lambda$ and $1.0\ \lambda$.

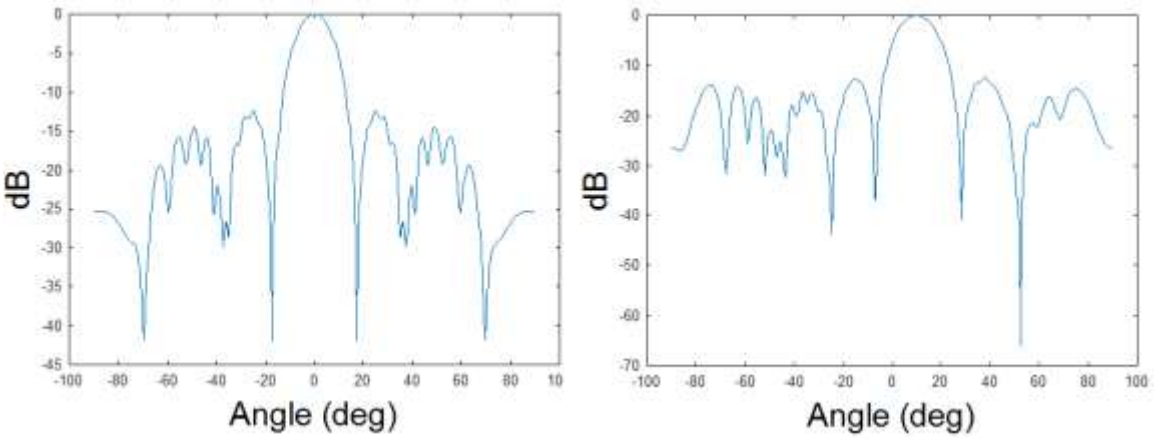


**Figure 3-6.**Radiation pattern for $P=3.2\ \lambda$ and $s_m=0.5\ \lambda$, $\theta=0,10$ degrees.

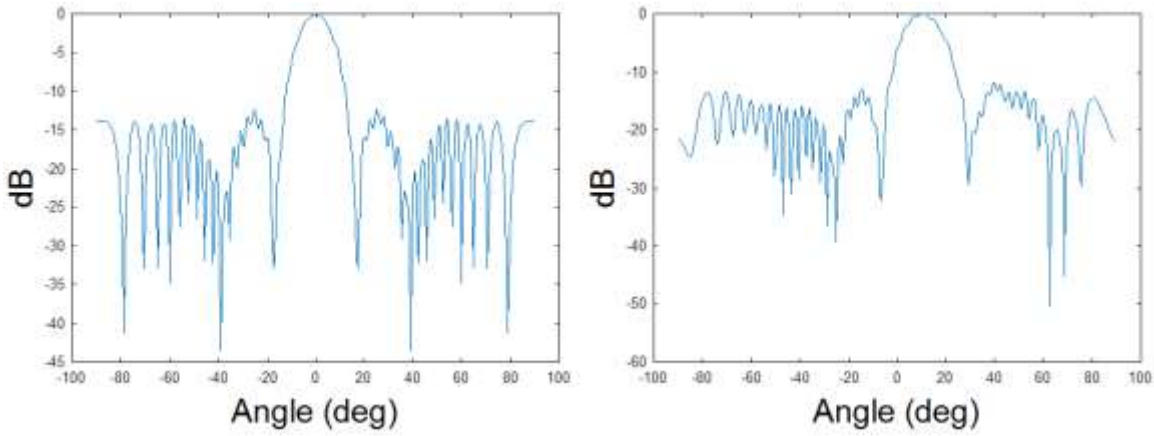


**Figure 3-7.**Radiation pattern for $P = 16\ \lambda$ and $s_m = 0.5\ \lambda$, $\theta = 0, 10$ degrees.

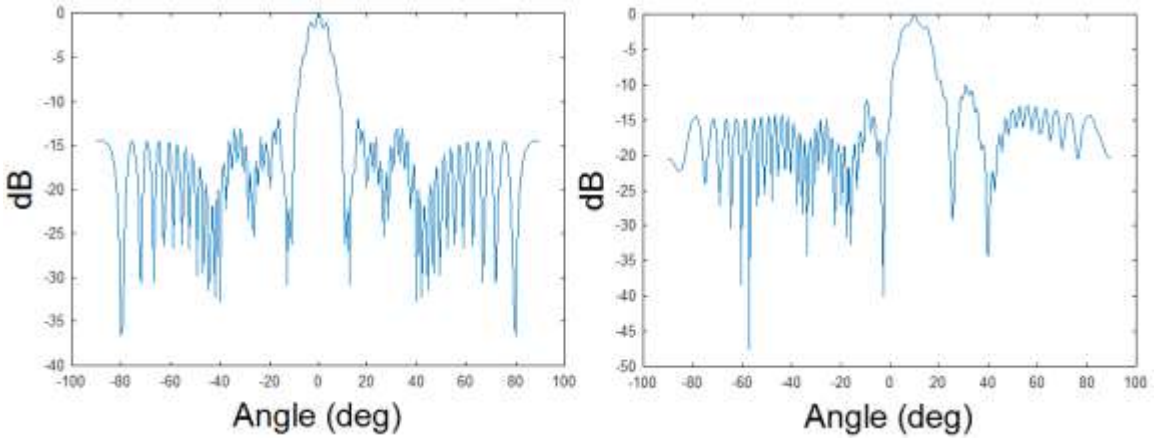


**Figure 3-8.**Radiation pattern for $P = 32\ \lambda$ and $s_m = 0.5\ \lambda$ , $\theta = 0, 10$ degrees.

#### 3.2.2.2 Aperiodic elements distributions of the SPAF

In the previous section, radiation pattern analysis was performed optimizing the excitation (phase $\emptyset_{fm}$ and magnitude $A_{fm}$) of a periodic SPAF (i.e., the spacing between its elements is the same). In this section, an aperiodic SPAF is analyzed to explore the advantages that can be obtained of the freedom degrees in an aperiodic linear array, where each active element has a different position $s_m$ (i.e., the spacing between its elements is different).

Remembering that DLA's design, according to McGrath's equations, assume that their active elements or excitation (i.e. the feeding) are in the focal arc. Thus, the positions of these elements depend on the $F$ focal length and the $\theta$ steering angle, $[\pm F \sin\theta\,, F\cos\theta]$. Since the SPAF is a linear array and the DLA was designed for a feeding in the focal arc, then the analysis is performed assuming that the aperiodic SPAF is an approximate linear projection on the y- axis of the active elements distributed in the focal arc, as shown in Figure 3-9.

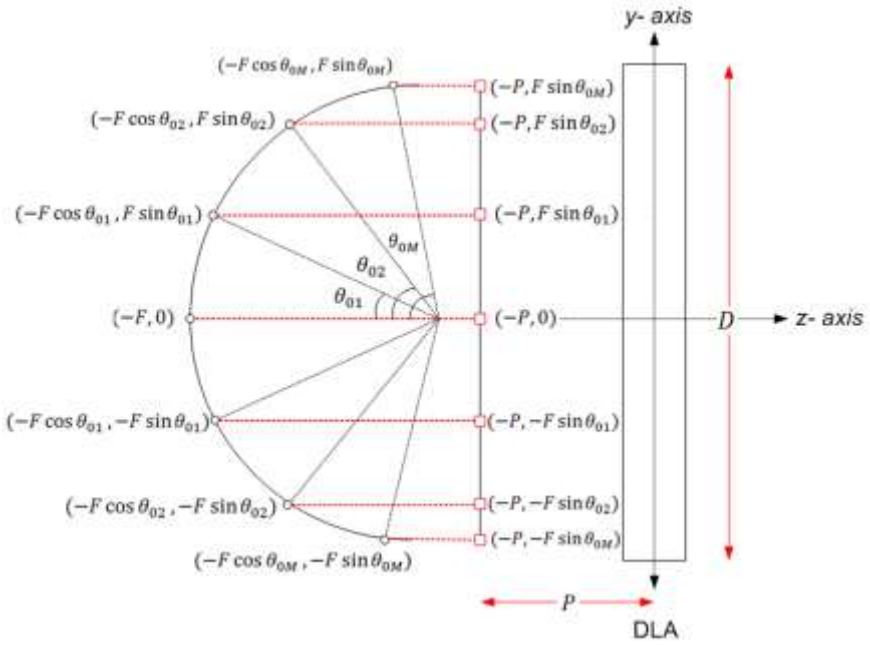


**Figure 3-9.**Small-Phased-Array-Fed SPAF and the feed side of the DLA as an aperiodic linear array.

In the case of the aperiodic SPAF its excitation (phase $\emptyset_{fm}$ and magnitude $A_{fm}$) has the same position $P$ on the z- axis, and position vector $s_m$ with two freedom degrees ($\alpha_m$ , $\theta_m$) on the y- axis, given in equations 3.17 and 3.18 respectively. In addition, parameter's value $P$ is fixed in the z- axis, in other words the active elements of the focal arc are fixed to a value choosing of $P$:

$$P \approx F\cos\theta \tag{3.17}$$

Given that $s_m$ (i.e. position vector of the elements on the y- axis) is an approximate linear projection of the active elements distributed in the focal arc, then $s_m$ is described in the following equation:

$$s_m = \pm\alpha_m \sin\theta_m \tag{3.18}$$

The active elements are symmetrically distributed on the y- axis from the z-axis (DLA center). Since SPAF cannot be larger than the DLA, and given that D is DLA's diameter, $\alpha_m$ takes values in the range of 0 to *D*/2. Parameter's values $\theta_m$ , varies in the range of values from $0^{\circ}$ up to $90^{\circ}$. Subsequently, the radiation patterns are calculated for each $s_m$ position vector using equations (3.1-3.11). The optimization is similar to that described in section 3.2.3; use the same equations of this section.

## 3.3 Synthesis method for obtaining the radiation pattern in the radiation side

In the previous sections the geometric description and the analysis of the proposed architecture are shown, and with these results a synthesis method is realized. This method of synthesis consists in the fact that, given a desired radiation pattern, the values of the parameters in the SPAF ($E_{fm}, s_m, M, P$) and DLA ($N$,$r_n, \theta_0$) are obtained. Then, the radiation pattern is first obtained from the DLA elements on the radiation side, since these elements form a linear array, as shown in Figure 3-10.

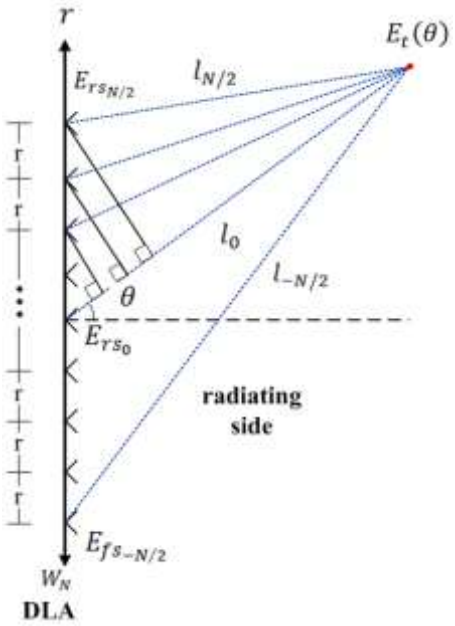


**Figure 3-10.**Radiation side of the DLA as a periodic linear array**.**

Dolph-Chebyshev synthesis method was used to calculate, $A_{fm}$, the amplitude of each element and the phase $\phi_{rsn}$ is calculated from the following equation:

$$\phi_{rsn} = -rk \sin\theta \tag{3.19}$$

Array pattern synthesis has a wide variety of techniques and methods. Many intricate procedures have been developed for synthesizing using array factors (AF), such as the method of Dolph-Chebyshev Weights [44, 45]. In addition, this method results in a radiation pattern with low side lobes, which is required in communication applications [45]. For instance, a PHA to generate low side lobe patterns, or accurate approximations of desired radiation patterns, just need to control its amplitude and phase [44]. Since an array synthesis is the reverse process of array analysis.

The method of Dolph-Chebyshev calculates the coefficients given elements number N+1 is equal 65, the spacing between elements 0.5 $\lambda$ and the ration SLL in dB. In Figure 3-12, is shown the radiation pattern for a steering angle $\theta$ equal to 0, 20, 40 degrees.

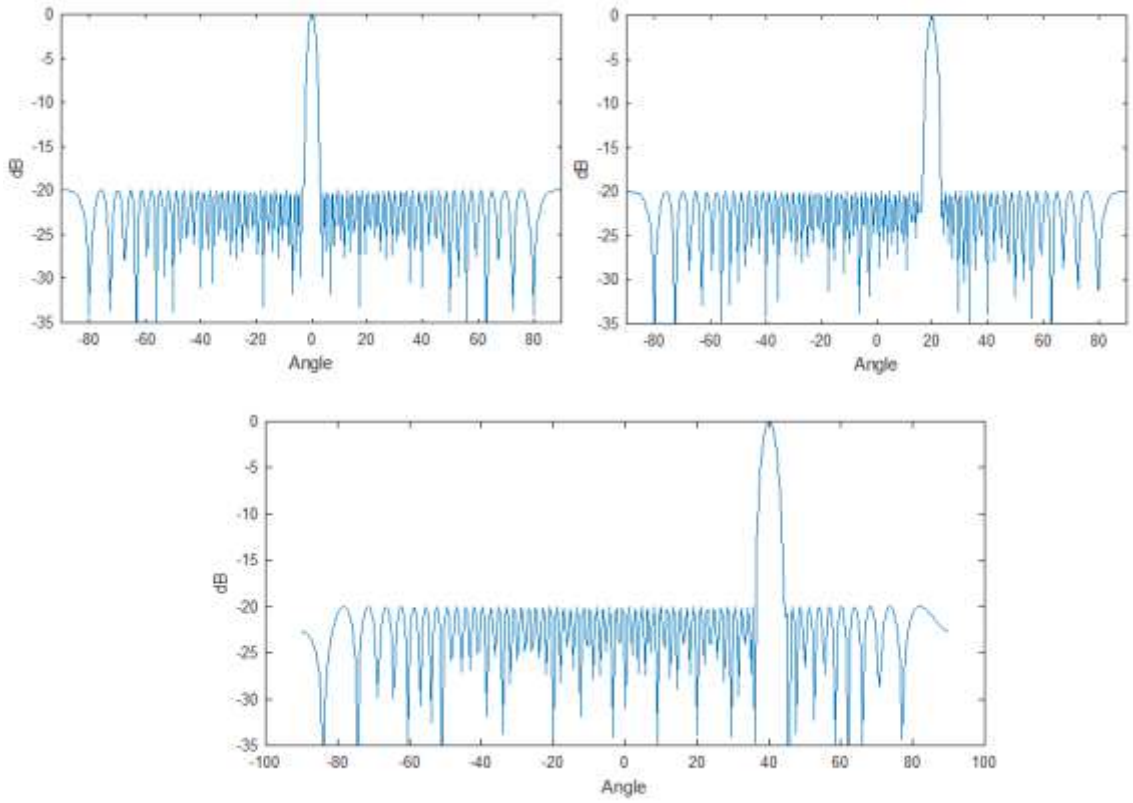


**Figure 3-11.**Radiation patterns generate by the method of Dolph-Chebyshev. for a steering angle $\boldsymbol{\theta}$ equal to 0, 20, 40 degrees.

With determined excitation values $E_{rsn}$ in the radiation side DLA, then the excitation values in the feed side are obtained $E_{fsn}$ of DLA (i.e. in the other face of the DLA) and for this it is only necessary to apply vector phase shift $W_n$, see equation 3.11 and Figure 3-12.

$$E_{fs_n} = E_{rs_n} {W_n}^{-1} \tag{3.20}$$

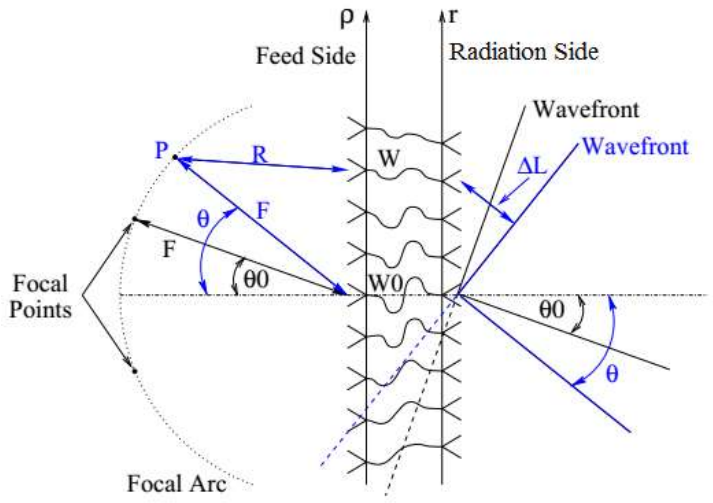


**Figure 3-12.**Geometry of DLA with its vector phase-shift $W_p$ for a steering angle $\theta$.

Continuing with the synthesis method in the feed side, to calculate the excitation in SPAF and the positions of their elements was used the method of QR decomposition, which consists in the solution de $N + 1$ equations with $M + 1$ variables. According to the novel architecture, its feed side can be expressed in matrix form as:

$$Ax = b \tag{3.21}$$

Where $A$ is a matrix that depend of $R_{mn}$,

$$A = \begin{bmatrix} \frac{e^{-jR_{11}}}{R_{11}} & \frac{e^{-jR_{21}}}{R_{21}} & \cdots & \frac{e^{-jR_{m1}}}{R_{m1}} \\ \frac{e^{-jR_{12}}}{R_{12}} & \frac{e^{-jR_{22}}}{R_{22}} & \cdots & \frac{e^{-jR_{m2}}}{R_{m2}} \\ \vdots & \vdots & \ddots & \vdots \\ \frac{e^{-jR_{1n}}}{R_{1n}} & \frac{e^{-jR_{2n}}}{R_{2n}} & \cdots & \frac{e^{-jR_{mn}}}{R_{mn}} \end{bmatrix} \tag{3.22}$$

Also, $x$ represents the excitation values in SPAF, i.e. $E_{fm}$, and $b$ is the electric field in the DLA's feed side,

$$x = \begin{bmatrix} E_{f1} \\ E_{f2} \\ \vdots \\ E_{fm} \end{bmatrix} \tag{3.23}$$

$$b = \begin{bmatrix} E_{fs1} \\ E_{fs2} \\ \vdots \\ E_{fsn} \end{bmatrix} \tag{3.24}$$

## 3.4 Algorithm in MATLAB

The next step will be the development of algorithms, based on previous equations (3.1-3.6), for generating the radiation pattern. Furthermore, one of the codes will optimize phase and magnitude of the feeder for each generated radiation pattern.

Additionally, it will perform the characterization of the new architecture by observing the radiation pattern, while it tracks the beam farther from broadside. The different combinations of the parameters, such as $P, s, M$, are taken into account, for characterization purposes.

Using the optimization code, excitation (phase and magnitude) will be obtained in the small-phased-array-fed for each combination of ( $P, s, M$).

Then, the optimization results will be the synthesis method, which will generate radiation patterns with main beam pointing at different angles to determine beam quality. For this case, Least Mean Squares (LMS) will also be used. The optimization component will be calculated within a MATLAB toolbox, using the functions fminsearch and fminunc.

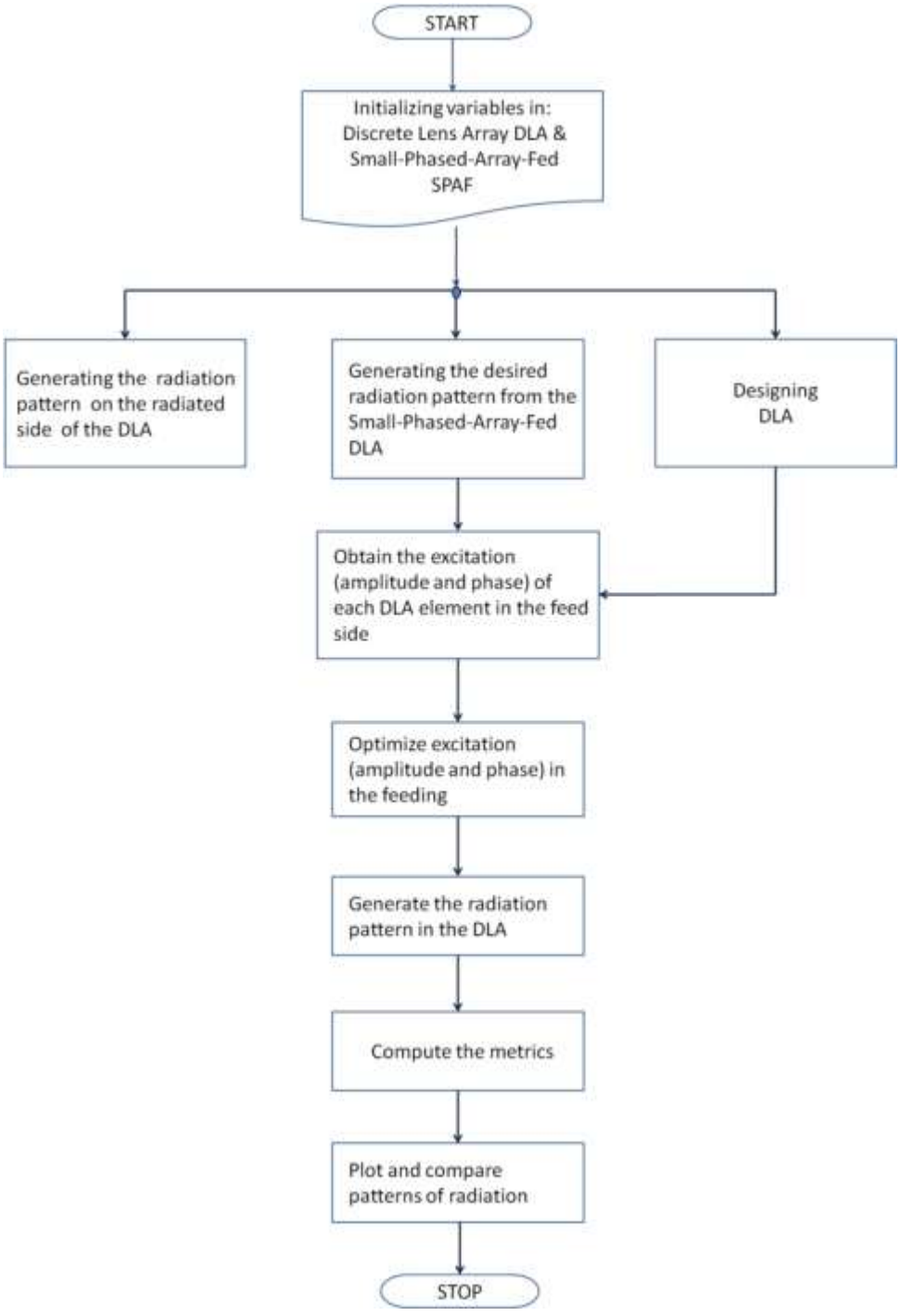


**Figure 3-13.**Diagram of the algorithm developed in MATLAB.

# 4 SIMULATIONS AND RESULTS

In this chapter, simulations and results of the characterization SPAF-DLA are described, and also, the comparison of the architecture SPAF-DLA as an alternative of low-cost with respect to linear phased array (PHA) and discrete lens array (DLA). The metrics previously defined in chapters (2) and (3) were used to measure the performance of SPAF-DLA, such as Gain (G), Side Lobe Level (SLL), Half-power beamwidth (3 dB beamwidth) or (HPBW) and Scanning Range (SR), which are shown in Figure 4-1,

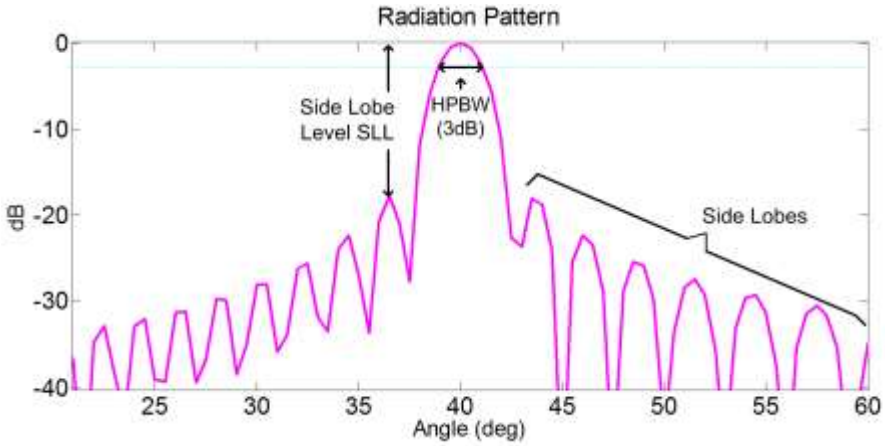


**Figure 4-1.**Metrics of an antenna array.

The DLA's design parameters values $(N, \theta_0, r)$ and the SPFA's parameters values $(M, P, s)$ are required for the simulations of the radiation patterns. Since that in section 3.2.1, the DLA's design parameters values $(N, r)$ are defined as $N + 1 = 65$, and $r_n =$

$n\lambda/2$. Thus, the characterization of the SPFA parameters $(M, P, s)$ are divided in two parts for a periodic SPAF and an aperiodic SPAF.

## 4.1 Simulations and results for a periodic Small-Phased-Array-Fed (SPAF)

In this case, the radiation pattern is obtained for a periodic Small-Phased-Array-Fed. Also, the initial value of $M$ is 7, to keep the array size about $N/10$, and $\theta_0$ is 20 degrees. Thus, the characterization of periodic SPAF-DLA is divided in two parts: first for the distance between SPAF and DLA and then the spacing among elements of SPAF.

### 4.1.1 Characterization the distance between SPAF and DLA

The characterization of the parameter $P$, which is the distance between SPAF and DLA, depends on the focal length $F$ of DLA. Also $p$ is the ratio between $P$ and $F$, $p$ can be expressed as follows:

$$p = {}^{P}/_{F}; \tag{4.1}$$

In Table 4.1, Scanning Range (SR) and Gain (G) decrease, and HPBW is more narrow, while $p$ increases from 0.1 to 1.0. If $p \geq 0.5$, the SR is less than 15 degrees. Also, if $p < 0.5$ the SLL is greater than 10.5 dB, but HPBW is more wide than 10 degrees.

**Table 4-1.**METRICS FOR $s = 0.5\,\lambda$

| $p$ | SR (deg) | G (dB) | | SLL(dB) | | HPBW (deg) | | Power | |
|---|---|---|---|---|---|---|---|---|---|
| | | Min. | Max. | Min. | Max. | Min. | Max. | Min. | Max. |
| **0.1** | $\pm 41.0$ | 8.8 | 10.0 | 5.6 | 6.2 | 18.0 | 21.0 | 6.0 | 6.4 |
| **0.2** | $\pm 41.0$ | 7.6 | 9.3 | 5.3 | 7.0 | 9.5 | 17.0 | 5.2 | 6.4 |
| **0.3** | $\pm 34.5$ | 6.4 | 7.2 | 5.6 | 7.0 | 9.5 | 14.5 | 4.5 | 6.1 |
| **0.4** | $\pm 25.5$ | 4.8 | 6.7 | 6.0 | 7.5 | 10.0 | 12.5 | 3.6 | 5.0 |
| **0.5** | $\pm 20.0$ | 2.5 | 5.1 | 5.9 | 6.3 | 7.0 | 10.0 | 3.1 | 4.3 |
| **0.6** | $\pm 15.5$ | 0.0 | 4.1 | 6.5 | 6.7 | 6.0 | 8.0 | 2.8 | 3.5 |
| **0.7** | $\pm 10.0$ | $-2.7$ | $-0.9$ | 5.4 | 6.9 | 4.0 | 6.0 | 3.5 | 4.3 |
| **0.8** | $\pm 10.0$ | $-6.8$ | $-2.2$ | 4.6 | 7.1 | 2.0 | 6.5 | 3.1 | 3.2 |
| **0.9** | $\pm 5.0$ | $-6.4$ | $-3.2$ | 3.4 | 9.0 | 2.0 | 4.0 | 2.9 | 3.3 |
| **1.0** | $\pm 5.0$ | $-3.8$ | 4.5 | 4.4 | 9.9 | 2.0 | 4.0 | 2.9 | 3.1 |

In Table 4.2, 4.3 and 4.4, the amplitudes and phases in the feeding are presented for Scanning Range (SR) equal to $\pm 30$ degrees and $\pm 40$ degrees. The amplitude was normalized and the phase is in degrees.

**Table 4-2.**METRICS FOR $p = 0.1$ or $P = 3.2\lambda$

| $\theta$ deg | Amplitude (dB) | | | | | | | Phase (degree) | | | | | | |
|---|---|---|---|---|---|---|---|---|---|---|---|---|---|---|
| | $E_{f1}$ | $E_{f2}$ | $E_{f3}$ | $E_{f4}$ | $E_{f5}$ | $E_{f6}$ | $E_{f7}$ | $E_{f1}$ | $E_{f2}$ | $E_{f3}$ | $E_{f4}$ | $E_{f5}$ | $E_{f6}$ | $E_{f7}$ |
| **0°** | .86 | 1.0 | .96 | .98 | .96 | 1.0 | .86 | 252 | 106 | 100 | 263 | 263 | 256 | 251 |
| **10°** | .89 | 1.0 | .98 | .97 | .98 | 1.0 | .86 | 329 | 306 | 277 | 245 | 211 | 165 | 131 |
| **20°** | .86 | .99 | .98 | .94 | 1.0 | .95 | .85 | 375 | 318 | 249 | 187 | 117 | 42 | 339 |
| **30°** | .94 | .90 | .96 | 1.0 | .97 | .88 | .88 | 9 | 283 | 191 | 92 | 314 | 242 | 148 |
| **40°** | .94 | .88 | .96 | 1.0 | .98 | .93 | .99 | 318 | 206 | 86 | 314 | 177 | 222 | 274 |

**Table 4-3.**METRICS FOR $p = 0.2$ or $P = 6.4\lambda$

| $\theta$ deg | Amplitude (dB) | | | | | | | Phase (degree) | | | | | | |
|---|---|---|---|---|---|---|---|---|---|---|---|---|---|---|
| | $E_{f1}$ | $E_{f2}$ | $E_{f3}$ | $E_{f4}$ | $E_{f5}$ | $E_{f6}$ | $E_{f7}$ | $E_{f1}$ | $E_{f2}$ | $E_{f3}$ | $E_{f4}$ | $E_{f5}$ | $E_{f6}$ | $E_{f7}$ |
| $0^{\circ}$ | .95 | .89 | 1.0 | .89 | 1.0 | .89 | .95 | 317 | 335 | 330 | 340 | 330 | 333 | 318 |
| $10^{\circ}$ | .89 | 1.0 | .98 | .98 | .96 | 1.0 | .89 | 30 | 1 | 329 | 292 | 253 | 210 | 166 |
| $20^{\circ}$ | .93 | .95 | .90 | .96 | 1.0 | .89 | .83 | 13 | 307 | 237 | 166 | 84 | 1 | 293 |
| $30^{\circ}$ | 1.0 | .86 | .72 | .76 | .90 | .98 | .97 | 257 | 150 | 47 | 308 | 196 | 73 | 310 |
| $40^{\circ}$ | .92 | .97 | 1.0 | .97 | .89 | .79 | .74 | 46 | 256 | 101 | 303 | 145 | 346 | 189 |

**Table 4-4.**METRICS FOR $p = 0.3$ or $P = 9.6\lambda$

| $\theta$ deg | Amplitude (dB) | | | | | | | Phase (degree) | | | | | | |
|---|---|---|---|---|---|---|---|---|---|---|---|---|---|---|
| | $E_{f1}$ | $E_{f2}$ | $E_{f3}$ | $E_{f4}$ | $E_{f5}$ | $E_{f6}$ | $E_{f7}$ | $E_{f1}$ | $E_{f2}$ | $E_{f3}$ | $E_{f4}$ | $E_{f5}$ | $E_{f6}$ | $E_{f7}$ |
| $0^{\circ}$ | .95 | .56 | 1.0 | .57 | 1.0 | .56 | .95 | 28 | 53 | 36 | 65 | 36 | 54 | 28 |
| $10^{\circ}$ | .98 | .78 | .91 | 1.0 | .7 | .98 | .94 | 87 | 47 | 26 | 328 | 290 | 252 | 185 |
| $20^{\circ}$ | .7 | .96 | .92 | .59 | .73 | 1.0 | .94 | 1 | 284 | 6 | 105 | 46 | 306 | 199 |
| $30^{\circ}$ | .63 | .5 | .62 | .85 | 1.0 | 1.0 | .90 | 76 | 334 | 229 | 101 | 320 | 176 | 32 |

Figure 4.2, 4.3 and 4.4, the radiation patterns shown that HPBW is more narrow and SR= $\pm 20$ degrees for $p = 0.5$ or $p = 16\lambda$. However, the Gain varies by more than 2 dB.

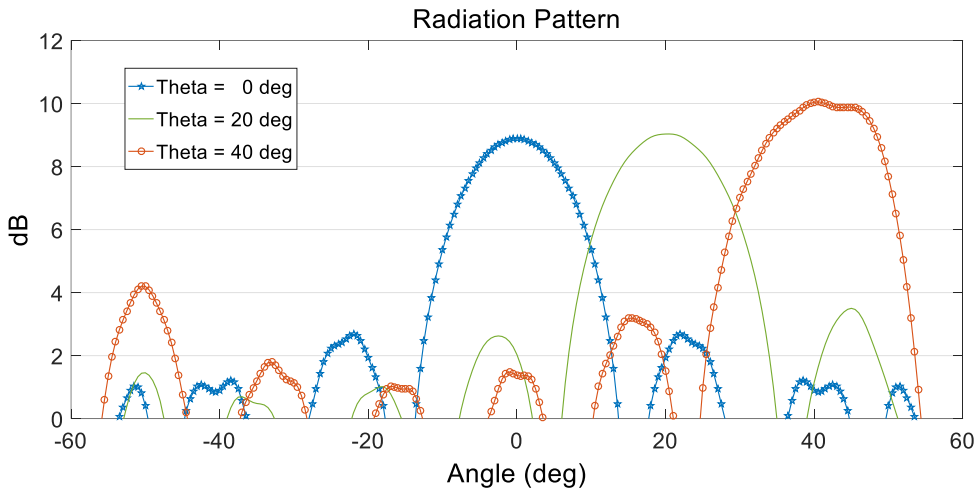


**Figure 4-2.**Radiation pattern for $p = 0.1$ or $P = 3.2\lambda$.

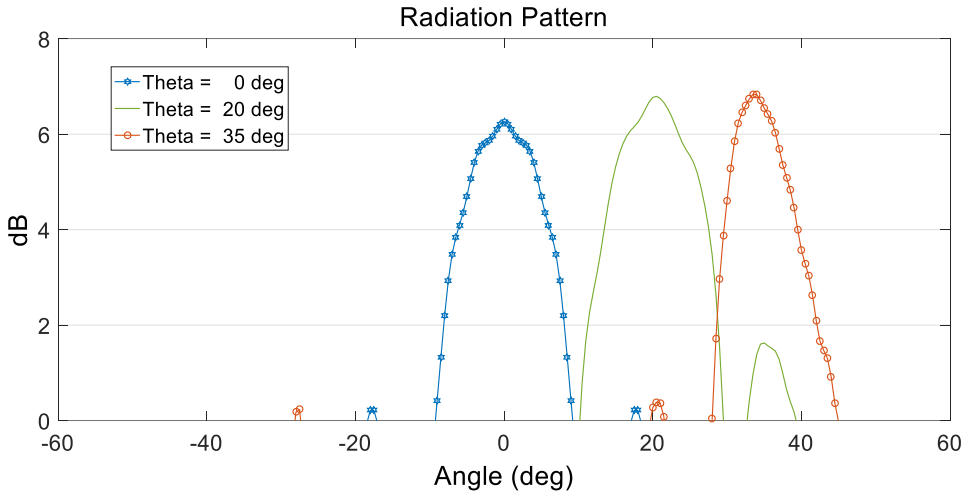


**Figure 4-3.** Radiation pattern for $p = 0.3$ or $P = 9.6\lambda$.

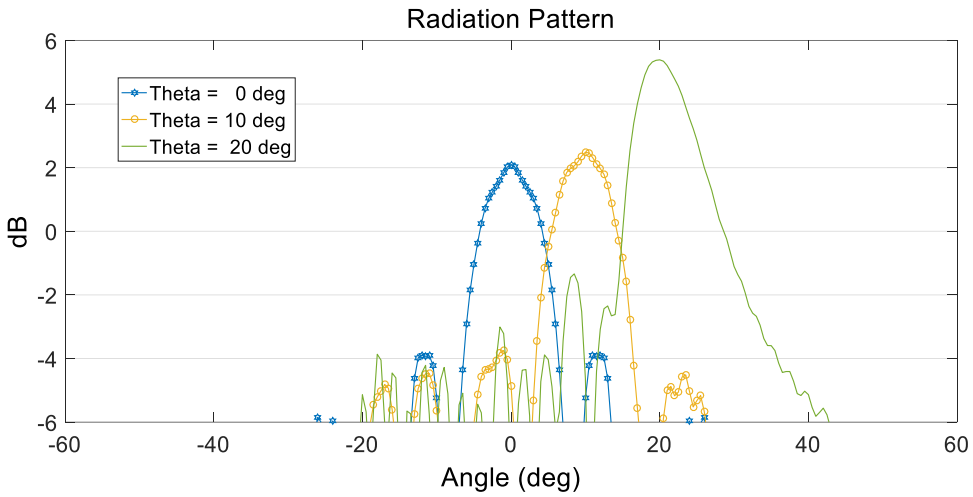


**Figure 4-4.** Radiation pattern for $p = 0.5$ or $P = 16.0\lambda$.

### 4.1.2 Characterization the spacing between elements of a periodic SPAF

From the previous section 4.1.1, given a $p = 0.3$ or $P = 9.6\lambda$, thus, SR is equal $\pm 35$ degrees and HPBW is in the range of 7 degrees to 14 degrees. Then, this $p$ value is used as a reference to evaluate the radiation pattern and characterize parameters values $s$, which is the spacing between the elements in the SPAF.

In Table 4.5, there is no significant variation of the Scanning Range (SR) according to the range of values of $s$. If $s$ takes the values between $0.1\lambda$ to $0.3\lambda$, thus, the Gain is negative, SLL is less than 2 dB, and HPBW can reach up to 25 degrees, as shown in Figure

4-5 and 4-6. If $s$ takes the values between $0.4\lambda$ to $0.7\lambda$, thus, the Gain is positive, SLL is greater than 2 dB, and HPBW decreases, as shown in Figure 4-7.

**Table 4-5.**METRICS FOR $p = 0.3$ or $P = 9.6\,\lambda$

| $s$ | SR (deg) | G (dB) | | SLL(dB) | | HPBW (deg) | | Power | |
|---|---|---|---|---|---|---|---|---|---|
| | | Min. | Max. | Min. | Max. | Min. | Max. | Min. | Max. |
| **0.1** | $\pm 35.0$ | $-7.5$ | $-1.8$ | 1.0 | 5.9 | 7.0 | 35.0 | 2.8 | 4.4 |
| **0.2** | $\pm 35.5$ | 0.0 | $-10.6$ | 1.3 | 5.3 | 7.0 | 25.0 | 2.2 | 4.2 |
| **0.3** | $\pm 36.5$ | $-8.2$ | $-2.1$ | 2.0 | 7.0 | 6.8 | 25.0 | 2.6 | 3.3 |
| **0.4** | $\pm 36.0$ | 0.4 | 5.1 | 3.9 | 6.5 | 8.0 | 18.0 | 3.1 | 4.8 |
| **0.5** | $\pm 34.5$ | 6.0 | 7.8 | 4.4 | 7.0 | 7.5 | 14.5 | 4.5 | 6.1 |
| **0.6** | $\pm 34.5$ | 5.8 | 7.2 | 1.5 | 6.3 | 11.5 | 12.5 | 2.9 | 6.6 |
| **0.7** | $\pm 35.0$ | 5.4 | 7.0 | 0.4 | 6.6 | 7.0 | 11.0 | 2.8 | 6.4 |
| **0.8** | $\pm 34.5$ | 5.6 | 6.8 | 0.5 | 6.5 | 6.5 | 9.5 | 2.6 | 5.6 |
| **0.9** | $\pm 36.5$ | 4.3 | 6.3 | 0.3 | 7.5 | 7.7 | 8.0 | 2.7 | 5.4 |
| **1.0** | $\pm 37.5$ | 4.2 | 6.7 | 0.0 | 5.3 | 7.7 | 8.0 | 2.7 | 5.7 |

Given that SR depends mainly on $P$. Thus, if $p = 0.3$ and $s = 0.5$ the radiation pattern generated a wide SR$= \pm 35$ degrees, a positive and stable and SLL$\geq$ 4.4 dB. However, if $s > 0.5\lambda$, SLL decreases, as shown in Figure 4-8 and 4.9.

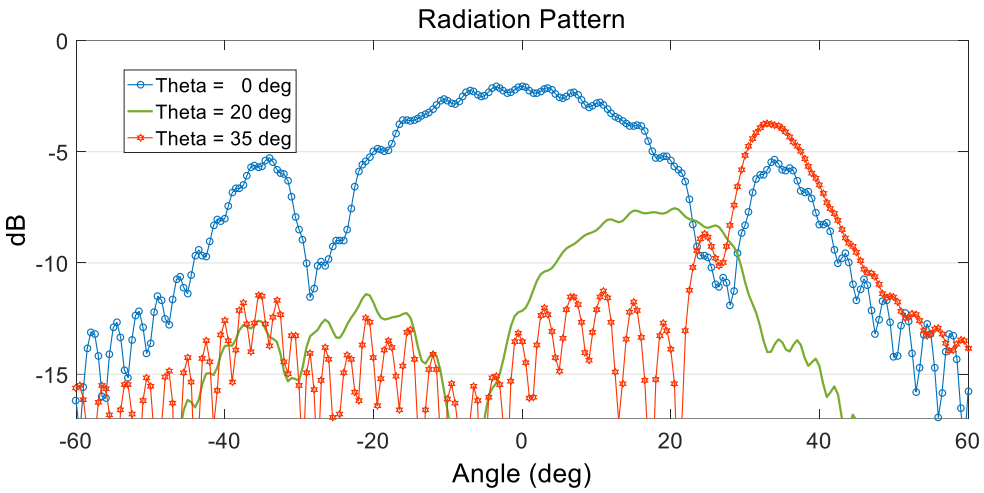


**Figure 4-5.**Radiation pattern for $s = 0.1\lambda$.

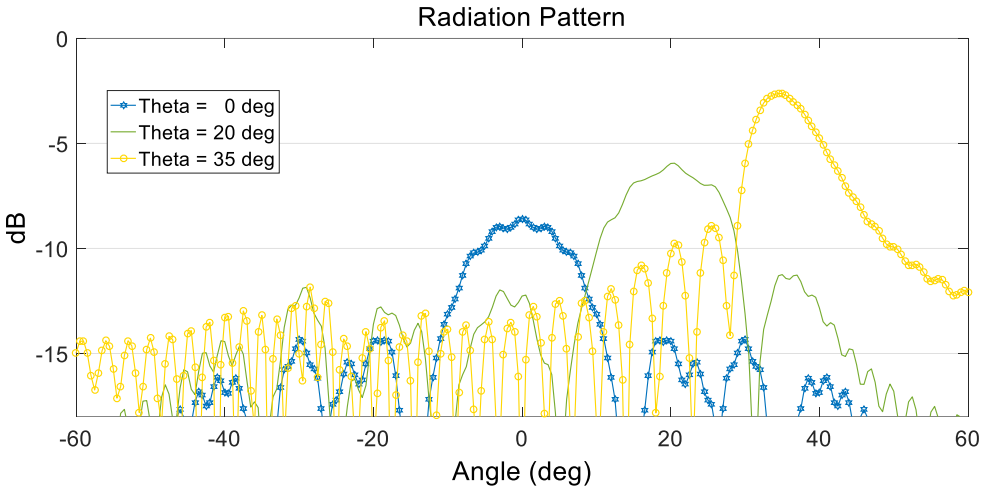


**Figure 4-6.**Radiation pattern for $s = 0.3\lambda$.

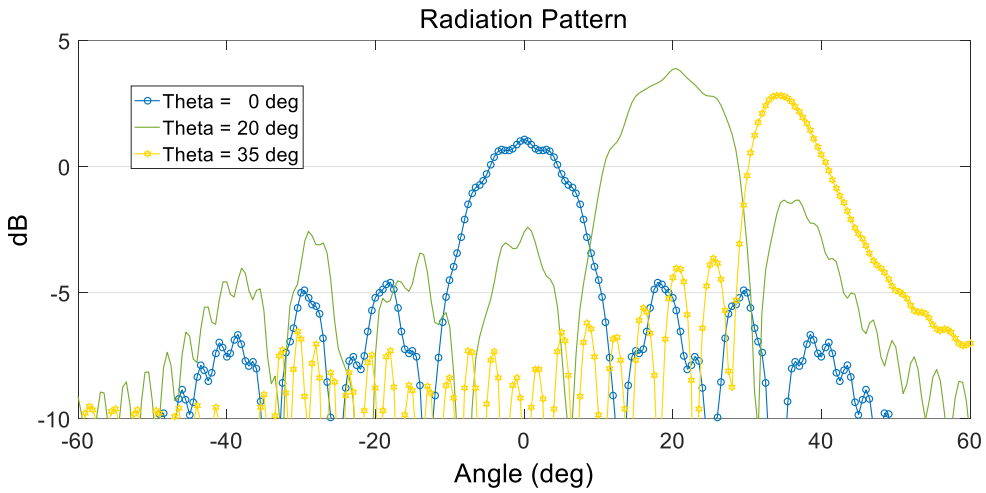


**Figure 4-7.**Radiation pattern for $s = 0.4\lambda$.

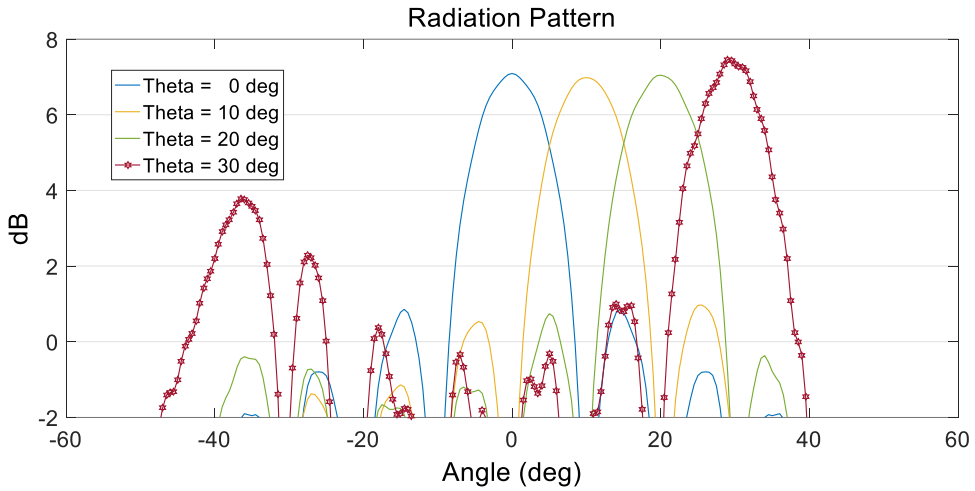


**Figure 4-8.**Radiation pattern for $s = 0.6\lambda$.

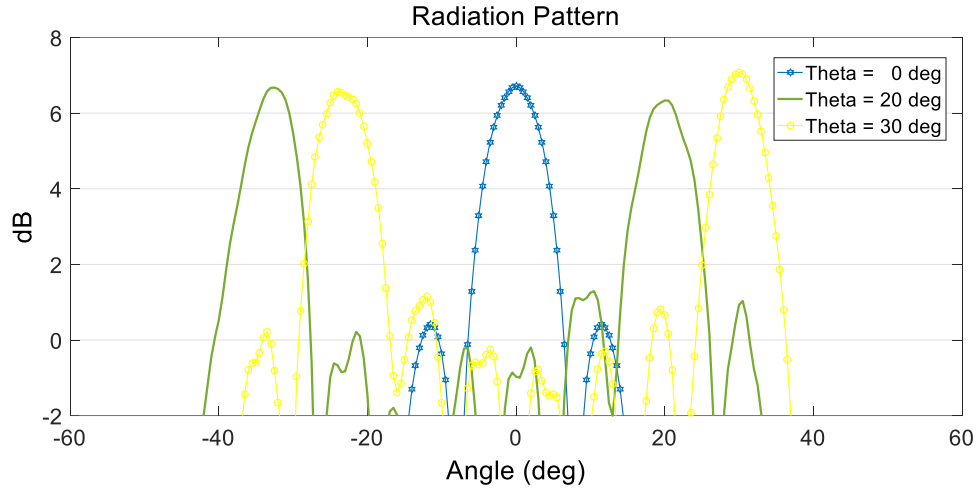


**Figure 4-9.**Radiation pattern for $s = 0.8\lambda$.

## 4.2 Simulations and results for an aperiodic Small-Phased-Array-Fed SPAF

The spacing between elements is evaluated in a sine function, which depends on the angle and amplitude. Given an amplitude equal to $8.0\lambda$ and an angle with progressive distribution equal to $0,\ 20,\ 40,\ 60$ degrees to generate the radiation pattern, as shown in the equations:

$$s = 8\lambda\left[-\sin(60^{\circ});\ -\sin(40^{\circ});-\sin(20^{\circ});\sin(0^{\circ});\sin(20^{\circ});\sin(40^{\circ});\sin(60^{\circ})\right] \quad (4.2)$$

$$s = [-6{,}928\lambda;\ -5{,}142\ \lambda;-2{,}736\ \lambda;\ 0;\ 2{,}736\ \lambda;\ 5{,}142\ \lambda;\ 6{,}928\ \lambda\ ] \quad (4.3)$$

Table 4.6 and 4.7 describe the metrics of the radiation pattern generated for $p = 0.5$ and $p = 0.3$ respectively, also spacing described in equations (4.2) and (4.3).

**Table 4-6.**METRICS FOR $\theta_0 = 20$ degrees, $p = 0.5$ or $P = 16\lambda$

| $\theta$ (deg) | SR (deg) | G (dB) | SLL(dB) | HPBW (deg) | POWER |
|---|---|---|---|---|---|
| **0°** | [0-29] | [24.3-22.2] | [1.6-3.6] | [1.0-5.0] | 2.7 |
| **20°** | [0-30] | [24.4-22.0] | [2.5-4.3] | [1.0-7.0] | 2.8 |
| **30°** | [0-32.5] | [24.0-22.7] | [1.0-3.9] | [1.0-3.5] | 3.2 |
| **40°** | [0-34.5] | [24.0-21.1] | [1.8-3.4] | [1.5-4.0] | 3.4 |

**Table 4-7.**METRICS FOR $\theta_0 = 20$ degrees, $p = 0.3$ or $P = 9.6\lambda$

| $\theta$ (deg) | SR (deg) | G (dB) | SLL(dB) | HPBW (deg) | POWER |
|---|---|---|---|---|---|
| **0°** | [0-37.5] | [21.2-23.0] | [1.6-4.0] | [2.0-4.0] | 1.7 |
| **20°** | [0-38.5] | [21.9-22.9] | [1.7-3.7] | [2.0-4.5] | 2.9 |
| **30°** | [0-40.0] | [21.9-22.5] | [2.0-4.0] | [2.0-4.0] | 2.3 |
| **40°** | [0-40.0] | [21.1-22.8] | [1.3-3.4] | [2.0-5.0] | 3.9 |

Characterization of $P$ by the following spacing between the elements:

$$s = 8\lambda\left[-\sin(86^{\circ});\ -\sin(54^{\circ});-\sin(27^{\circ});\sin(0^{\circ});\sin(27^{\circ});\sin(54^{\circ});\sin(86^{\circ})\right] \quad (4.4)$$

$$s = [-7{,}981\lambda;\ -6{,}472\lambda;-3{,}632\lambda;\ 0;\ 3{,}632\lambda;\ -6{,}472\lambda;\ -7{,}981\lambda\ ] \quad (4.5)$$

Table 4.8 describes the metrics of the radiation pattern generated for $p = 0.3$ respectively, also spacing described in equations (4.4) and (4.5).

**Table 4-8.**METRICS FOR $\theta_0$ degrees and $p = 0.3$ or $P = 9.6$.

| $\theta$ (deg) | SR (deg) | G (dB) | SLL(dB) | HPBW (deg) | POWER |
|---|---|---|---|---|---|
| **0°** | [0-38.5] | [21.9-22.7] | [1.0-4.8] | [1.0-3.5] | 2.5 |
| **20°** | [0-39] | [21.8-22.9] | [1.7-6.0] | [1.0-3.5] | 2.1 |
| **30°** | [0-41] | [22.1-24.1] | [3.0-4.8] | [1.0-4.0] | 2.7 |
| **40°** | [0-40] | [21.0-21.9] | [3.5-5.0] | [1.0-5.0] | 3.1 |

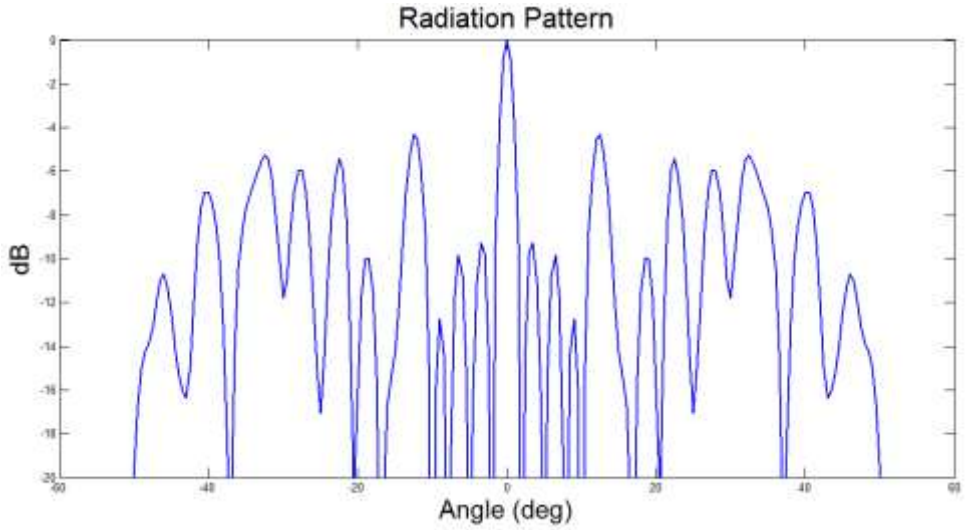


**Figure 4-10.**Radiation pattern for a small-phased-array-fed aperiodic for $\theta = 0$ degrees and $p = 0.3$ or $P = 9.6\ \lambda$.

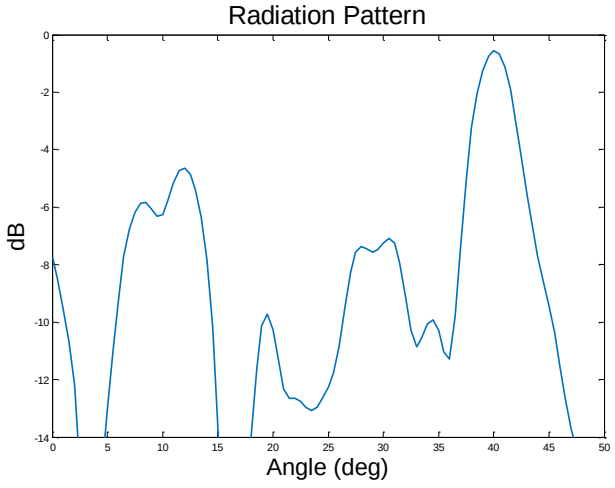


**Figure 4-11.**Radiation pattern for a small-phased-array-fed aperiodic for $\theta = 40$ degrees and $p = 0.3$ or $P = 9.6\ \lambda$.

Figure 4-12, show the radiation patterns for $\theta_0 = 30$ degrees, with scan range from 0 up to 40 degrees, where $s$ is the position of the feeding equation (4.5).

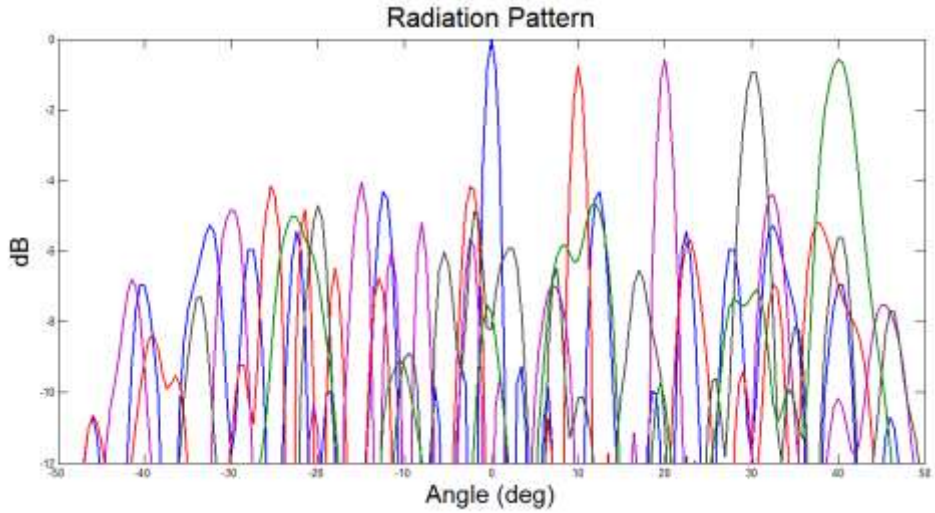


**Figure 4-12.**Radiation pattern for a small-phased-array-fed aperiodic for $\theta = 0$ degrees up to $\theta = 40$ degrees and $p = 0.3$ or $P = 9.6\lambda$.

## 4.3 Comparing SPAF-DLA, Phased Array and DLA

In this section, SPAF-DLA, Phased Array (PHA) and Discrete Lens Array (DLA) are compared using the SR, D, SLL, and HPBW metrics. Additionally, there are a comparison of costs and power consumed by the active elements. To perform the simulation of the PHA's radiation pattern, it is calculated for a number of elements equal to 65 elements with spacing between of 0.5λ and with maximum amplitude of 1.0. The simulation results are shown in Figure 4-13 and Figure 4-14.

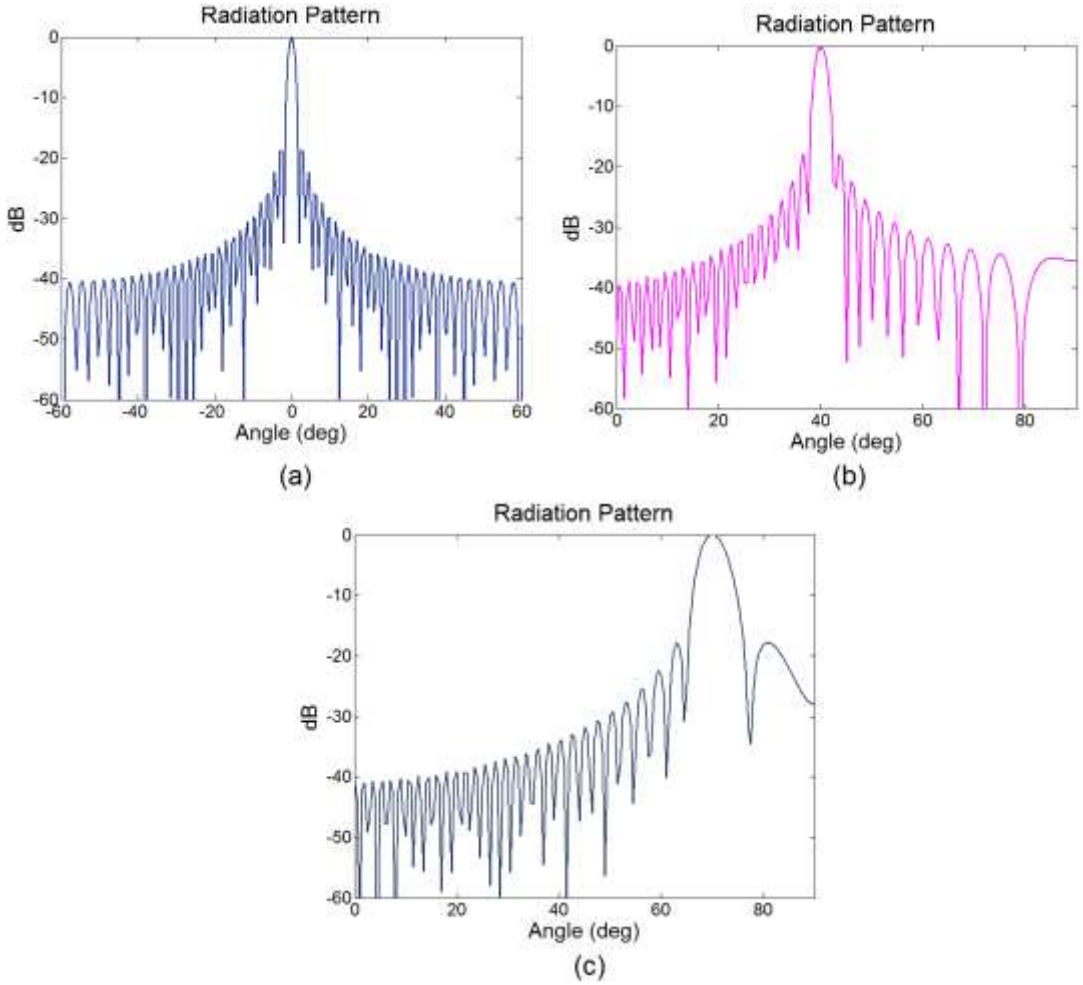


**Figure 4-13.**Radiation pattern for a phased array for: (a) $\theta = 0$ degrees; (b) $\theta = 40$ degrees; (c) $\theta = 70$ degrees.

**Table 4-9.**METRICS FOR A PHASED ARRAY OF 65 ELEMENTS.

| **θ (deg)** | **G (dB)** | **SLL (dB)** | **HPBW (deg)** | **POWER** |
|---|---|---|---|---|
| **0°** | 20.6 | 9.24 | 2.5 | 65 |
| **20°** | 20.3 | 9.48 | 2.5 | 65 |
| **40°** | 20.5 | 9.42 | 2.5 | 65 |
| **60°** | 20.6 | 9.41 | 3.0 | 65 |
| **78°** | 20.6 | 9.43 | 13.0 | 65 |

Table 4-9 describes the metrics of the radiation pattern generated by phased array, where a SR is displayed from $\pm 78$ degrees. With respect to the increase of HPBW, it happens when the point of the angle moves away broadside. The minimum value of HPBW being 2.5 degrees and the maximum of 13 degrees, and SLL decreases.

Table 4-10, 4-11 and 4-12, shows the metrics of the radiation pattern for different values of $\theta_0 = 20$, 30 and 40 degrees, which are plotted in the Figure 4-13 and 4-15. This architecture was described in chapters 2 and 3. For each point of interest a fixed element is needed in the focal arc. For instance, a scanning range from $0$ up to $10$ degrees, each 2 degrees, thus we need 6 elements that would point at the angles of $0, 2, 4, 6, 8, 10$ degrees. Therefore, to have a sweep of $\pm 40$ degrees, there are 41 elements in the focal arc. The difference with respect to the Phased Array PHA is that because it is in the focal arc it does not need a phased shifter and this reduces in $30\%$ costs.

The position of each element obeys the equation (4.6), and it will depend on where the point of interest is located. If the point of interest is $\theta$ degrees from z- axis, then the position is calculated as follows:

$$Position = (-F\cos\theta\,, \pm F\sin\theta) \tag{4.6}$$

**Table 4-10.**METRICS FOR $\theta_0 = 20$ degrees

| θ (deg) | G (dB) | SLL (dB) | HPBW (deg) | Power |
|---|---|---|---|---|
| **0°** | 2.9 | 4.3 | 2.5 | 1 |
| **10°** | 2.7 | 5.1 | 1.5 | 1 |
| **20°** | 2.6 | 7.2 | 1.5 | 1 |
| **30°** | 1.2 | 6.5 | 5.5 | 1 |
| **37°** | 0.8 | 6.4 | 13.0 | 1 |

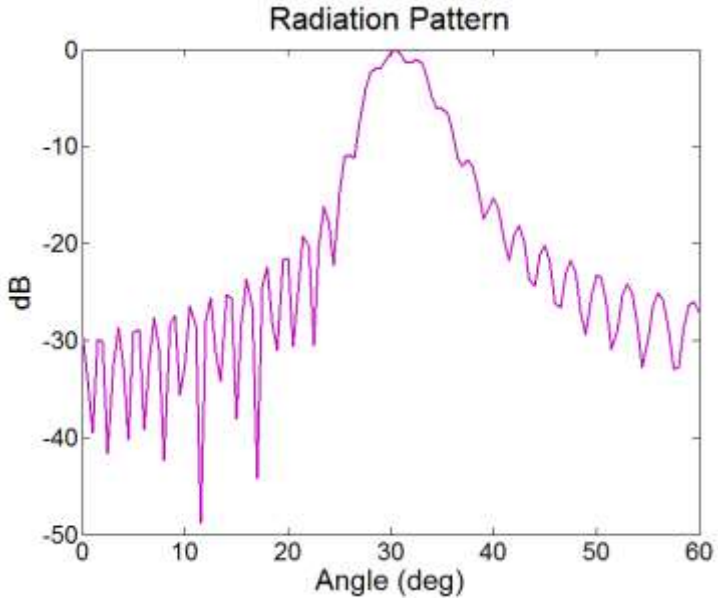


**Figure 4-14.**Radiation pattern for a DLA for $\theta_0 = 20$ degrees.

**Table 4-11.**METRICS FOR $\theta_0 = 30$ degrees

| $\theta$ (deg) | G (dB) | SLL (dB) | HPBW (deg) | POWER |
|---|---|---|---|---|
| **0°** | 1.2 | 5.0 | 9.0 | 1 |
| **10°** | 2.0 | 4.9 | 10.0 | 1 |
| **20°** | 2.6 | 5.9 | 7.0 | 1 |
| **30°** | 2.9 | 7.1 | 2.5 | 1 |
| **39°** | 2.8 | 6.2 | 4.0 | 1 |

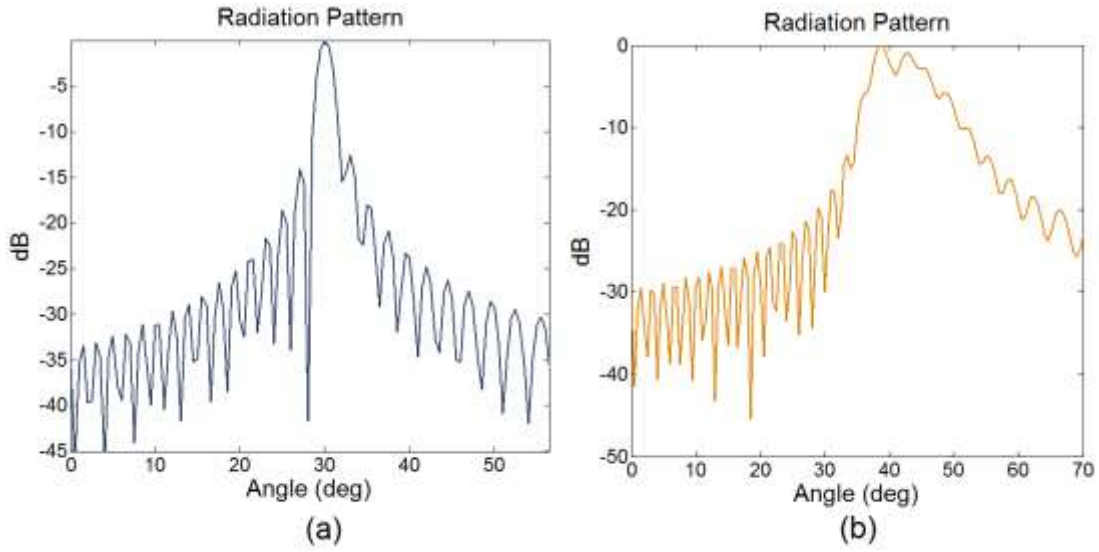


**Figure 4-15.**Radiation pattern for a DLA for $\theta_0 = 30$ degrees; (a) $\theta = 30$ degrees; (b) $\theta = 40$ degrees.

**Table 4-12.**METRICS FOR $\theta_0 = 40$ degrees

| $\theta$ (deg) | G (dB) | SLL (dB) | HPBW (deg) | Power |
|---|---|---|---|---|
| **0°** | 0.8 | 5.1 | 8.0 | 1 |
| **10°** | 1.5 | 6.4 | 10.0 | 1 |
| **20°** | 2.4 | 5.8 | 6.0 | 1 |
| **30°** | 2.3 | 5.5 | 5.0 | 1 |
| **40°** | 2.8 | 7.0 | 2.5 | 1 |
| **49°** | 2.2 | 0.7 | 2.0 | 1 |

Finally, after performing the analysis and description of each architecture, in Table 4-13, PHA, DLA and SPAF-DLA are compared. PHAs have extensive SR, it also maintains an HPBW equal to 1.5 degrees for a SR $\pm 80$ degrees.

**Table 4-13.**METRICS FOR PHA, DLA AND SPAF-DLA.

| | SR (deg) | G (dB) | SLL (dB) | HPBW (deg) |
|---|---|---|---|---|
| **PHASED ARRAY** | $\pm 78$ | 20.24 | 9.5 | [2.5-13] |
| **DISCRETE LENS ARRAY** | $\pm 37$ | 2.9 | [6-7] | [2.5-10] |
| **PERIODIC SPAF-DLA** | $\pm 45$ | 7.1 | [4-7] | [7.5-14] |
| **APERIODIC SPFA-DLA** | $\pm 35$ | 7.8 | [3-6] | [1.5-4.0] |

Table 4-14 describes power, # elements, costs. Assuming that the cost of each element active (i.e. transceiver) is $300. Then, the cost of the PHA would be $19,500. In the case of DLA, as it does not have phased shifter the cost would be $5,153 and for SPFA-DLA is $880.

**Table 4-14.**COMPARING POWER, # ELEMENTS AND COSTS FOR PHA, DLA AND SPAF-DLA.

| | POWER | # ELEMENTS | COSTS |
|---|---|---|---|
| **PHASED ARRAY** | 65 | 65 | $19,500 |
| **DISCRETE LENS ARRAY** | 1 | 41 | $5,153 |
| **PERIODIC SPAF-DLA** | 3 | 7 | $880.00 |
| **APERIODIC SPFA-DLA** | 3 | 7 | $880.00 |

# 5 CONCLUSION AND FUTURE WORK

## Conclusions

- Development of two synthesis methods for the characterization of the proposed architecture SPAFDLA.
- Array Performance Metrics were described.
- The power distribution analysis was performed.
- The mathematical modeling was presented for the design of the architecture SPAF-DLA.
- A toolbox was generated for the characterization of an architecture SPAF-DLA composed by a Phased Array and Discrete Lens Array.
- Analysis of the SPAF-DLA architecture, which reduces costs in comparison with PHA and DLA. Being low cost, the SPAF-DLA architecture is accessible to investigations of limited scanning range.
- In addition, SPAF-DLA is simple construction alternative unlike DLA has a difficult designed because of the focal arc architecture (where it locates its active elements).

## Future Work

- Because of the complexity of many variables optimizer, work focused on the characterization performed in one-dimension; however, small-phased-array fed SPAF-DLA can be explored and analyzed in 2-D and 3-D.
- Since work was based on characterizing the small-phased-array-fed DLA, then the investigation did not focus on looking for the best optimization method. Therefore, it would be important to compare different optimization methods mainly feeding.
- Small-phased-array-fed was analyzed as a linear array, and the optimization was performed on the z axis. Then, in search of improving the radiation pattern (i.e. SLL); one could optimize the distribution of components of SPAF on the y- axis.
- The QR decomposition method can be used to vary the dimensions of the proposed architecture.
- Emulation in HFSS software and implementation of architecture

# REFERENCES

[1] R. C. Hansen, Phased Array Antennas. 2009.

[2] R. J. Mailloux, Phased Array Antenna Handbook. 2005.

[3] W. Yao and Y. E. Wang, “Beamforming for phased arrays on vibrating apertures,” IEEE Trans. Antennas Propag., vol. 54, no. 10, pp. 2820–2826, 2006.

[4] D. McGrath, “Planar three-dimensional constrained lenses,” IEEE Trans. Antennas Propag., vol. 34, no. 1, pp. 46–50, 1986.

[5] E. W. Bryerton, M. D. Weiss, and Z. Popovic, “A 10-GHz high-efficiency lens amplifier array,” 1998 IEEE MTT-S Int. Microw. Symp. Dig. (Cat. No.98CH36192), vol. 3, pp. 1461–1464, 1998.

[6] S. Hollung and Z. B. Popovic, “A bi-directional active lens antenna array,” IEEE Antennas Propag. Soc. Int. Symp. 1997. Dig., vol. 1, pp. 26–29, 1997.

[7] J. L. Salazar, E. Loew, and P. Tsai, “Design Trade-offs for Airborne Phased Array Radar for Atmospheric Research,” pp. 371–378.

[8] S. Space, F. Lens, L. A. Ground, and S. Applications, “Steerable Space Fed Lens Array for Low-Cost Adaptive Ground Station Applications,” pp. 2136–2139, 2007.

[9] D. Popovic and Z. Popovic, “Multibeam antennas with polarization and angle diversity,” IEEE Trans. Antennas Propag., vol. 50, no. 5, pp. 651–657, 2002.

[10] S. Romisch, D. Popovic, N. Shino, R. Lee, and Z. Popovic, “Multi-Beam Discrete Lens Arrays with Amplitude-Controlled Steering,” Microw. Symp. Dig. 2003 IEEE

MTT-S Int., vol. 3, pp. 1669–1672, 2003.

[11] W. E. Kock, “Metal-Lens Antennas,” Proc. IRE, vol. 34, no. 11, pp. 828–836, 1946.

[12] V. R. Lakshmi and G. S. N. Raju, “Optimization of Radiation Patterns of Array Antennas,” pp. 1434–1438, 2011.

[13] J. Lipor and S. Ahmed, “Closed Form Fourier-Based Transmit Beamforming for MIMO Radar,” University of Michigan, Ann Arbor, King Abdullah University of Science and Technology, no. 1, pp. 5309–5313, 2014.

[14] J. Lizarraga, G. Crespo, and C. Del-Rio, “Discrete lenses for multibeam applications,” 5th Eur. Conf. Antennas Propagation, EUCAP 2011, pp. 3513–3517, 2011.

[15] B. Marcelo and E. Silvio, “A Multiple Beam Antenna System using Discrete Lens Arrays,” vol. 00001, pp. 3–6.

[16] R. V. McGahan, “A lens-array limited scan antenna,” Aperture, vol. 4.

[17] M. B. Perotoni, S. Rondineau, R. Lee, D. Consonni, and Z. Popovic, “X-band discrete lens array for a satellite communication ground station antenna,” SBMO/IEEE MTT-S Int. Microw. Optoelectron. Conf. Proc., pp. 197–200, 2005.

[18] L. Schwartzman, “Analysis of phased array lenses,” Antennas Propagation, IEEE, vol. 5611, pp. 628–632, 1968.

[19] R. M. Shubair and A. Hakam, “Adaptive Beamforming Using Variable Step-Size LMS Algorithm with Novel ULA Array Configuration.”

[20] U. Singh, “Linear Array Synthesis Using Biogeography,” Prog. Electromagn.

Res. M, vol. 11, pp. 25–36, 2010.

[21] Y. Tajima and Y. Yamada, “Gain and radiation pattern improvement in scanning beams of a shaped dielectric lens antenna by employing a patch array feed,” 2008 IEEE Int. Symp. Antennas Propag. Usn. Natl. Radio Sci. Meet. APSURSI, no. 1, pp. 2–5, 2008.

[22] C. Tang, “A dual lens antenna for limited electronic scanning,” 1975 Antennas Propag. Soc. Int. Symp., vol. 13, pp. 117–120, 1975.

[23] J. A. Torres-Rosario, S. Rondineu, R. A. Rodríguez-Solís, S. Hunt, and Z. Popovic, “Adaptive discrete lens antenna array for direction of arrival detection,” IEEE Antennas Propag. Soc. AP-S Int. Symp., vol. 4 A, pp. 122–125, 2005.

[24]J. Vian and Z. Popovic, “Smart lens antenna arrays,” Ieee Mtt S Int Microw. Symp Dig, vol. 3, pp. 129–132, 2001.

[25] P. Wenig and R. Weigel, “Analysis of a microstrip patch array fed cylindric lens antenna for 77GHz automotive radar,” 2008 IEEE Antennas Propag. Soc. Int. Symp., pp. 1–4, 2008.

[26] B. P. M. Woodward and J. D. Lawson, “RADIATION-PATTERN MAY BE OBTAINED FROM A SOURCE OF FINITE SIZE,” no. 2, 1948.

[27] Y. Yamada, N. Michishita, and S. Kamada, “Construction of wide angle beam scanning lens antenna and its applications,” 2009 Int. Conf. Sp. Sci. Commun., no. October, pp. 41–46, 2009.

[28] Sajid Ahmed and Mohamed-Slim Alouini, “A Waveform Covariance Matrix for

high SINR and Low Side-Lobe Levels," Computer, Electrical, and Mathematical Science and Engineering (CEMSE) Division King Abdullah University of Science and Technology (KAUST) Thuwa, Sci. Technol., pp. 4096–4100, 2013.

[29] Stefania Römisch, Paul C. Smith, Darko Popovic, Dana Z. Anderson, and Zoya Popovic, "A Lens Antenna Array with Adaptive Optical Processing Edeline Fotheringham", IEEE TRANSACTIONS ON ANTENNAS AND PROPAGATION, VOL. 50, NO. 5, MAY 2002.

[30] Juan A. Torres-Rosario, Sebastien Rondineu, Rafael A. Rodriguez-Solis, Shawn Hunt, Zoya Popovic; "Adaptive Discrete Lens Antenna Array for Direction of Arrival Detection", 2005 IEEE.

[31] National Center for Atmospheric Research. Available: https://ncar.ucar.edu/. [Accessed: March. 15, 2017].

[32] The National Severe Storms Laboratory. Available: http://www.nssl.noaa.gov/about/history/nwrt-decommission/. [Accessed: Feb. 5, 2017].

[33] MWR-05XP Mobile Phased Array Weather Radar. Available: http://cirpas.org/mobileRadarTruck.html . [Accessed: Dec. 12, 2016].

[34] Gary Louis Rait, **"**Quasi-Optical Discrete Lens Arrays for Synthetic Aperture Radar", Thesis Doctoral, CU Boulder, 2002.

[35] M. A. Mangoud and H. M. Elragal, "Antenna Array Pattern Synthesis and Wide Null Control Using Enhanced Particle Swarm Optimization", Progress In Electromagnetics Research B, Vol. 17, 2009.

[36] Marcelo B. Perotoni, Sébastien Rondineau, Richard Lee, Denise Consonni, Zoya Popovic, "X-band discrete lens array for a satellite communication ground station antenna", 2005 IEEE.

[37] Zoya Popovic, Stefania Romisch and Sebastien Rondineau, "Multibeam Phased

Array Antennas," Final report, Department of Electrical and Computer Engineering University of Colorado at Boulder, Boulder, CO 80309.
[38] U. Singh, H. Kumar, T. S. Kamal, "Linear Array Synthesis Using Biogeography Based Optimization," Progress in Electromagnetics Research M, Vol. 11, 25, 2010.
[39] R. J. Abad, M. H. Ierkic and E. I. Ortiz-Rivera, "Basic understanding of cognitive Radar," *2016 IEEE ANDESCON*, Arequipa.
[40] P. Ge, G. Cui, S. M. Karbasi, L. Kong and J. Yang, "Cognitive radar sequence design under the spectral compatibility requirements," in IET Radar, Sonar & Navigation, vol. 11, no. 5, pp. 759-767, 5 2017.
[41] Mary AM Ingram, Robert Romanofsky, Q. Lee, Zoya Popovi, John Langley, William C. Basott, M. Usman Ahrned, and Dan Mandl, "Optimizing Satellite Communications with Adaptive and Phased Array Antennas," Department of Electrical and Computer Engineering University of Colorado at Boulder, Boulder.
[42] R. Abad, R. Huertas, F. Arias, "Analysis and Design of FFT Algorithms Using Group Theory and Kronecker Products," 2015 Computing Alliance for Hispanic-Serving Institutions (CAHSI) – September 10-12, 2015, San Juan, Puerto Rico.
[43] M. S. Greco, F. Gini and P. Stinco, "Cognitive radars: Some applications," 2016 IEEE Global Conference on Signal and Information Processing (GlobalSIP), Washington, DC, 2016, pp. 1077-1082.
[44] Y. M. Madany, H. M. Elkamchouchi and A. E. Ahmed, "Smart distributed subarray MIMO (DS-MIMO) microstrip antenna system with frequency agile for communication and radar applications," 2016 Loughborough Antennas & Propagation Conference (LAPC), Loughborough, 2016, pp. 1-5.
[45] B. K. Lau and Y. H. Leung, "A Dolph-Chebyshev approach to the synthesis of array patterns for uniform circular arrays," 2000 IEEE International Symposium on Circuits and Systems. Emerging Technologies for the 21st Century. Proceedings (IEEE Cat No.00CH36353), Geneva, 2000, pp. 124-127 vol.1.